

# Optimal hydrogen supply chains: co-benefits for integrating renewable energy sources

Fabian Stöckl<sup>\*†</sup>, Wolf-Peter Schill<sup>\*‡</sup>, Alexander Zerrahn<sup>\*</sup>

May 22, 2020

## Summary

Green hydrogen can decarbonize transportation, but also help to integrate variable renewable energy sources if its production is sufficiently flexible in time. Using an open-source co-optimization model of the power sector and four supply chains for hydrogen at filling stations, we find a trade-off between energy efficiency and temporal flexibility: for lower shares of renewables and hydrogen, more energy-efficient decentralized electrolysis is optimal. For higher shares of renewables and/or hydrogen, more flexible centralized hydrogen supply chains gain importance as they allow disentangling hydrogen production from demand via storage. Liquid hydrogen emerges as particularly beneficial, followed by liquid organic hydrogen carriers and gaseous hydrogen. Centralized hydrogen supply chains can deliver substantial power sector co-benefits, mainly through reduced renewable surplus generation. Energy modelers and system planners should consider the flexibility characteristics of hydrogen supply chains in more detail when assessing the role of green hydrogen in future energy transition scenarios.

*Keywords:* hydrogen supply chains, LOHC, power sector modeling, renewable integration

---

<sup>\*</sup>German Institute for Economic Research (DIW Berlin), Germany.

<sup>†</sup>Technische Universität Berlin, Germany.

<sup>‡</sup>Energy Transition Hub, University of Melbourne, Australia.

# 1 Introduction

The increasing use of renewable energy sources in all end-use sectors is a main strategy to reduce greenhouse gas emissions [1]. Beyond current electricity use, energy demand from other sectors such as transportation may be satisfied either directly by renewable electricity or indirectly by hydrogen and derived synthetic fuels produced with renewable electricity [2, 3, 4, 5]. The potential of hydrogen-based electrification for deep decarbonization is widely acknowledged [6, 7, 8, 9, 10]. Yet, evidence is scarce so far how such electrification, also referred to as sector coupling, impacts the power sector, and, conversely, how conditions in the power sector impact sector coupling strategies.

We tackle this research gap by investigating different supply chains of hydrogen. Importantly, these supply chains imply a flexibility-efficiency trade-off: more energy-efficient options tend to be temporally less flexible, mainly because of more expensive storage, and more flexible options tend to be less energy-efficient (see Figure SI.12). Thus, hydrogen supply chains differ both with respect to their additional demand for renewable electricity and their temporal flexibility, with respective implications for the power sector. We investigate this trade-off in an analysis on the use of hydrogen for road-based passenger mobility. Specifically, we examine least-cost options for the supply of electrolysis-based hydrogen at filling stations in future scenarios with high shares of variable renewable electricity. To this end, we use an open-source optimization model with a well-to-tank perspective that co-optimizes alternative hydrogen supply chains and the power sector. We apply the model to German 2030 scenarios that vary the shares of renewable energy sources in electricity generation and the demand for hydrogen.

Our main contribution is evidence on the benefits of different hydrogen supply chains in a power sector with high shares of renewable energy sources. Most previous power sector analyses that include a hydrogen sector lack detail to discuss different hydrogen production and distribution options [11, 12, 13, 14, 15]. Studies that include more techno-economic details of supply chains for (green) hydrogen mobility often rely on exogenous electricity price assumptions, include only rudimentary power sectors, and/or are restricted to a single supply channel [16, 17, 18, 19, 20, 21, 22].

Methodologically, we extend the established open-source power sector model DIETER with a detailed representation of four hydrogen supply chains. The model minimizes the overall costs of the integrated electricity-hydrogen sectors, comprising both fixed and variable costs. Hydrogen may be produced with small-scale decentralized electrolyzers at filling stations or with large-scale centralized electrolyzers (Figure 1). In the latter case, hydrogen is distributed as liquid hydrogen ( $\text{LH}_2$ ), compressed gaseous hydrogen ( $\text{GH}_2$ ) or using a liquid organic hydrogen carrier (LOHC, see [23]). Available production technologies are proton exchange membrane (PEM) and alkaline (ALK) water electrolysis.

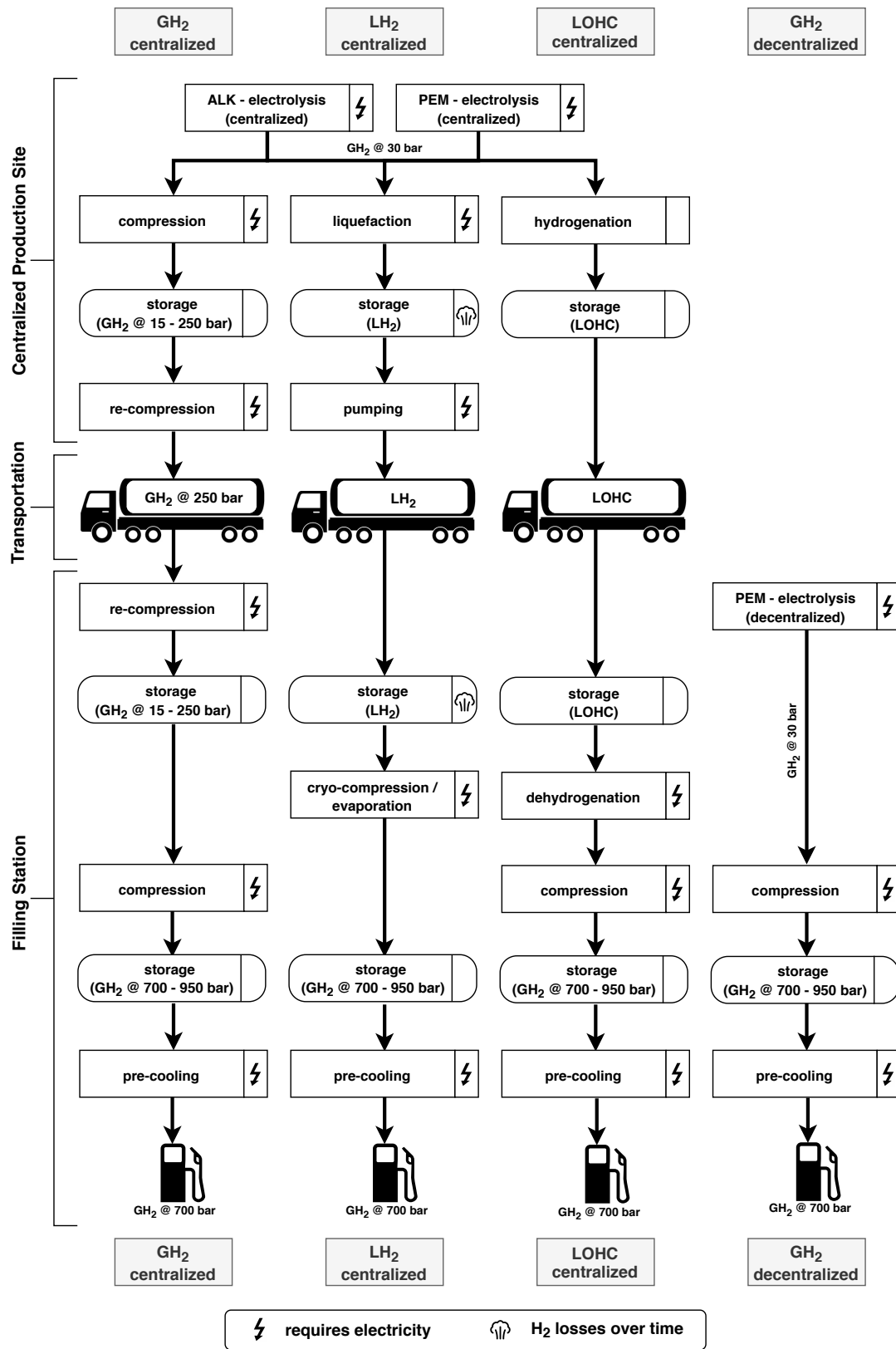


Figure 1: Centralized and decentralized supply chains with specific production, processing, transportation, and storage requirements.

The four supply chains differ, first, in their temporal flexibility. The centralized options allow for large-scale hydrogen storage, while the decentralized option only comes with a short-term buffer storage at the filling station. Second, they differ in how much electricity is required and when.  $\text{LH}_2$  requires a substantial amount of electricity after electrolysis for liquefaction. LOHC also has a high electricity demand to provide heat for dehydrogenation, but this takes place after  $\text{H}_2$  transportation and storage. Decentralized electrolysis at the filling station is the most energy-efficient option because it requires less electricity-intensive compression and conversion steps (for an illustration see [SI.3](#)).

Endogenous model variables comprise all electricity generation and storage capacities, their hourly dispatch, as well as capacity and hourly use decisions for the hydrogen supply chains. Exogenous model inputs include cost and efficiency parameters for all technologies as well as time series of electricity demand, hydrogen demand, and renewable energy availability. To adequately capture the variability of renewable energy sources, we solve the model for all 8760 consecutive hours of a year, assuming a long-run first-best equilibrium perspective. Section [4.1](#) provides details on the model setup. For transparency and reproducibility, model code and all input data are available under a permissive open-source license.

We parameterize the model to a 2030 setting for Germany. As the German government repeatedly committed itself to an ambitious expansion of renewable energy sources and currently also promotes the use of green hydrogen, it constitutes a relevant case study. To explore drivers of results, 12 scenarios vary the shares of renewable energy sources in electricity generation between 65-80 % in five percentage points increments and the demand for hydrogen between 5, 10, and 25 % of private and public road-based passenger vehicle energy demand. For each renewable share, we also devise a respective baseline without hydrogen demand. A renewable share of 65 % matches the target of the current German government for 2030. Larger shares allow to learn about higher ambition levels. The annual hydrogen demands are 9.1, 18.1 and 45.3  $\text{TWh}_{\text{H}_2}$  (272, 544, and 1359 kt) at the filling stations and allow to learn about the impact of an extended market penetration. We denote the resulting renewables-demand scenarios as *Res65-Dem5*, *Res65-Dem10*, and so on.

To address the trade-off between flexibility and energy efficiency, we combine the decentralized hydrogen supply option with each of the three centralized options for each scenario. We restrict model runs to three combinations per scenario for two reasons. First, we do not expect parallel infrastructures for centralized technologies to emerge in a plausible future setting. This is due to path dependencies and technology specialization that we cannot represent in the model. Second, discarding implausible technology combinations substantially reduces the computational burden.

## 2 Results

### 2.1 Optimal hydrogen supply chains depend on renewable penetration and hydrogen demand

Figure 2 shows the cost-minimal combinations of decentralized and centralized hydrogen supply chains for the 12 scenarios with hydrogen demand. It also shows the Additional System Costs of Hydrogen (ASCH, defined in Section 4.2).

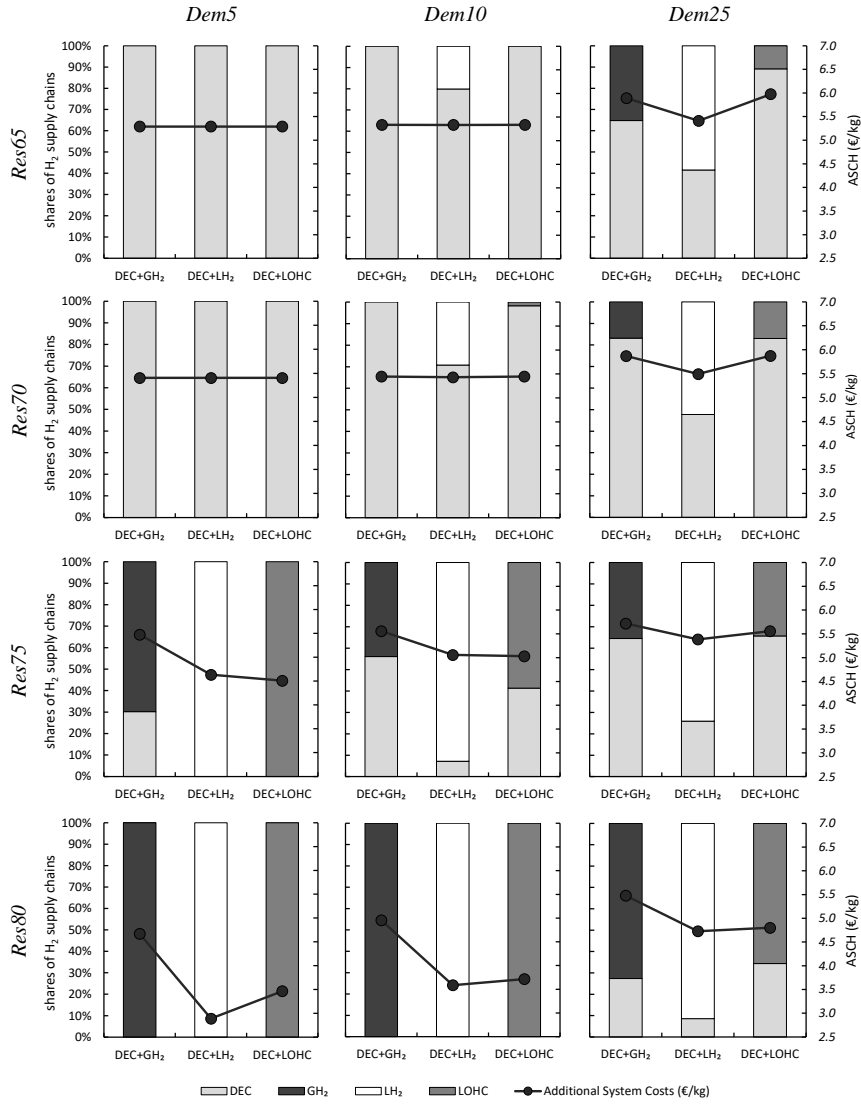


Figure 2: Optimal combinations of decentralized and centralized hydrogen supply chains and Additional System Costs of Hydrogen (ASCH) for the 12 scenarios. Starting from the top left panel, the share of renewable energy sources increases to the bottom, and the demand for hydrogen increases to the right.

For combinations of relatively low shares of renewable energy sources (65-70 %) and hydrogen demand (5-10 % of road-based passenger traffic), decentralized electrolysis is the least-cost option. That is, the energy efficiency benefits of decentralized electrolysis prevail over the flexibility benefits of the centralized options. Centralized supply chains increasingly become part of the optimal solution for higher shares of renewables or larger hydrogen demand. In these scenarios, the flexibility they offer becomes more valuable. Among the three centralized options, liquid hydrogen tends to have the largest shares in the optimal solution.

Comparing the Additional System Costs of Hydrogen, the solutions that include compressed gaseous hydrogen are always dominated by liquid hydrogen and often also by LOHC. This is because  $\text{GH}_2$  incurs comparably high storage and transportation costs (see [SI.3](#)). In contrast, solutions that include  $\text{LH}_2$  lead to the lowest ASCH in most scenarios with high renewable shares (75-80 %) or high hydrogen demand (25 %). In general, solutions that include  $\text{LH}_2$  or LOHC often lead to relatively similar cost outcomes. Yet, this is driven by different underlying mechanisms, i.e., higher overall energy efficiency of  $\text{LH}_2$  and higher temporal flexibility of LOHC (see Section [2.2](#) and [SI.3](#)).

Further, the additional system costs of hydrogen generally increase with hydrogen demand and decrease with the share of renewable energy sources, mainly reflecting the availability of cheap renewable surplus energy (see Section [2.3](#)).

## 2.2 Use patterns of hydrogen production and storage indicate differences in temporal flexibility

Differences in hydrogen storage capabilities as well as the level and timing of electricity demand ([SI.3](#)) lead to very different utilization patterns of the four hydrogen supply chains. We illustrate this for the optimal combination of decentralized electrolysis and  $\text{LH}_2$  in the *Res80-Dem25* scenario.

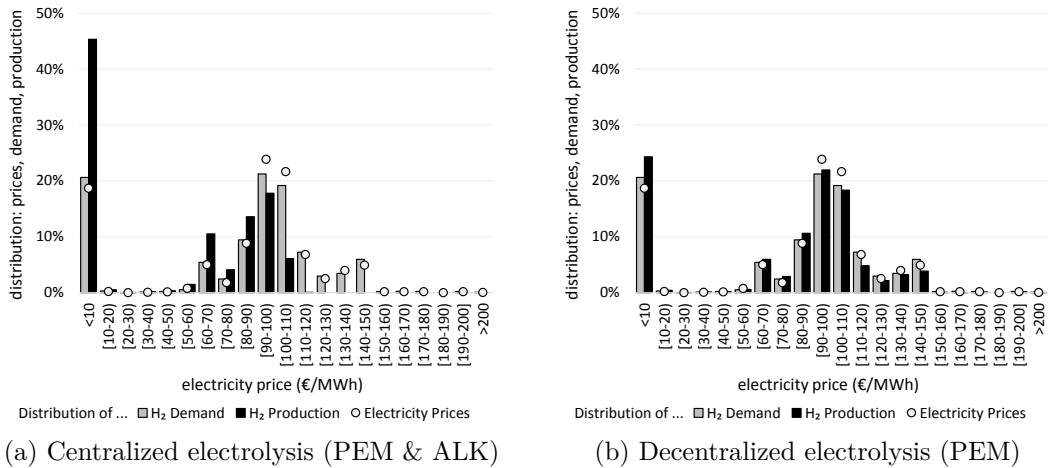


Figure 3: Distribution of hydrogen production, hydrogen demand, and electricity prices, exemplary for DEC+ $\text{LH}_2$  in scenario *Res80-Dem25*

Figure [3a](#) shows that  $\text{LH}_2$  allows to temporally disentangle hydrogen produc-

tion from demand. On average, production is high in hours when (renewable) electricity is abundant and, thus, cheap. These are not necessarily hours of high hydrogen demand. At the filling station, dispensing centrally produced LH<sub>2</sub> on time requires only little electricity. Vice versa, centralized hydrogen production is low in hours of high prices. In contrast, decentralized electrolysis only includes a small high-pressure buffer storage and needs to produce almost on demand (Figure 3b). Thus, through greater temporal flexibility, centralized supply allows to exploit phases of low electricity prices, which can overcompensate the overall higher electricity demand. Comparable production patterns emerge also for the other two centralized supply chains GH<sub>2</sub> and LOHC.

The capacities of production site hydrogen storage and its hourly use vary substantially across the three centralized options (Figure 4). LOHC has the highest overall storage capacity and a strongly seasonal use pattern. In contrast, GH<sub>2</sub> has a much smaller storage capacity and a pronounced short-term storage pattern. LH<sub>2</sub> storage is in between. Capacity deployment of GH<sub>2</sub> storage is small because of its relatively high specific investment costs. This changes in a sensitivity with cheap cavern storage (see SI.1.3). For LH<sub>2</sub>, storage investment costs are much lower, yet investment costs for liquefaction plants are high, impeding investments in larger LH<sub>2</sub> production capacities. LH<sub>2</sub> storage is also subject to a small, but relevant boil-off, which makes it less suitable for long-term storage. For LOHC, both investment costs for storage and hydrogenation plants are relatively low and investments, accordingly, high. As there is also no boil-off, LOHC storage is used for seasonal balancing.

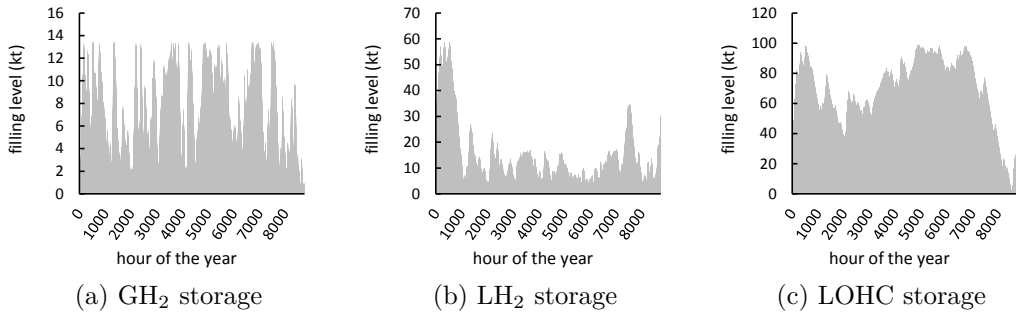


Figure 4: Temporal use pattern of production site storage in scenario *Res80-Dem25*

## 2.3 Power sector outcomes illustrate drivers for optimal hydrogen supply chains

Figure 5 summarizes power sector capacity impacts for the scenarios. Each bar shows the difference of optimal generation capacities compared to the respective baseline without H<sub>2</sub> demand. Generally, overall generation capacity increases with growing hydrogen demand and decreases with growing renewable penetration. A higher renewable share leads to higher renewable surplus generation. Centralized electrolyzers make use of this surplus that would otherwise be curtailed. In fact, in scenarios *Res80-Dem5* and *Res80-Dem10*, overall electricity

generation capacity hardly increases or even decreases because the additional electricity demand for hydrogen production is covered by renewable electricity that would otherwise not be used.

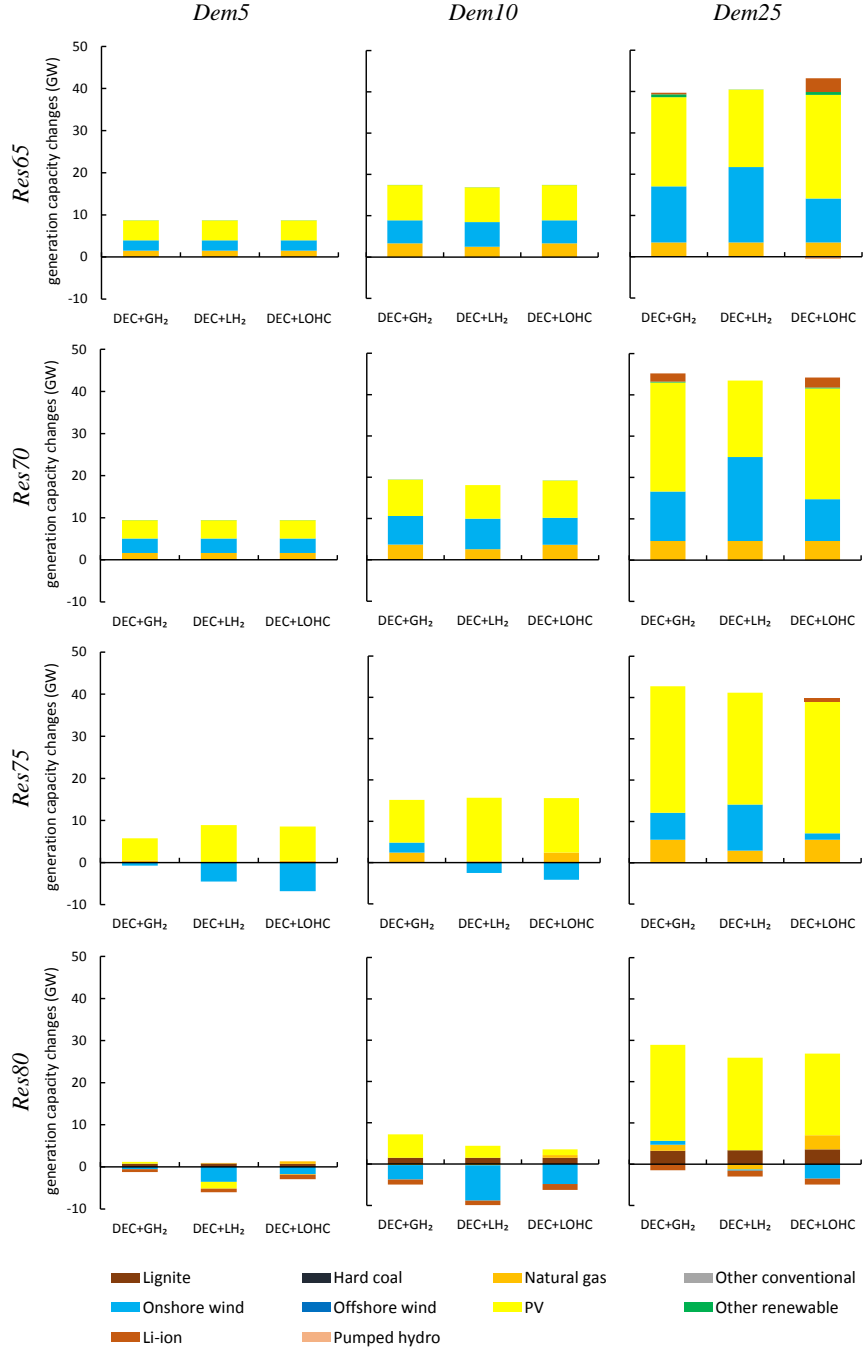


Figure 5: Electricity generation capacity changes compared to the respective baselines without hydrogen for optimal combinations of decentralized and centralized hydrogen supply chains as shown in Figure 2.



Concerning specific technologies, the additional electricity demand for hydrogen supply yields larger optimal solar PV capacities. Additional investments in wind power are lower, and the optimal wind power capacity even decreases in some *Res75* or *Res80* scenarios compared to the respective baseline. Additional wind power would lead to more sustained renewable surplus events, which would be harder to integrate. Offshore wind power is always deployed at the exogenous lower capacity bound of 17 GW. We further find a slight increase in the natural gas generation capacity in most scenarios because this is the most economical conventional generation technology to be operated with relatively low full-load hours. Compared to the respective baselines, the supply of hydrogen further tends to increase the optimal electricity storage capacity in the scenarios with lower renewable penetration because inflexible decentralized hydrogen production prevails here. In contrast, the optimal electricity storage capacity decreases in the *Res80* scenarios. Here, centralized hydrogen supply chains add a substantial amount of flexibility to the power sector.

Figure 6 shows the impact of hydrogen supply chains on yearly energy generation. Across scenarios, wind power is a major source of the additional electricity required for hydrogen supply. Much of this wind power would be curtailed in a power sector without hydrogen. The central driver for this result is that centralized hydrogen supply chains allow to make better use of variable renewable energy sources, facilitated through longer-term storage. In the *Res75* and *Res80* scenarios, electricity generation from wind turbines increases substantially although wind capacity hardly increases or even decreases (compare Figure 5). Renewable curtailment decreases most in scenario *Res80-Dem25* with LOHC, where full-load hours of wind power increase by 19 %. LOHC has the largest capability to integrate renewable surpluses by means of storage and also requires the largest amount of electricity.

Power generation from conventional generators also increases and supplies that part of the additional electricity that is not covered by renewables according to the specified share. In the *Res65-Dem25* and *Res70-Dem25* scenarios with largely inflexible, decentralized electrolysis, this is mainly natural gas-fired power generation. With increasing shares of renewables, there is a shift to hard coal and lignite. In *Res80-Dem25*, the share of lignite in non-renewable power generation is highest. Here, the temporal flexibility of centralized hydrogen supply chains allows increasing the full-load hours of conventional generation with the highest fixed and lowest variable costs, i.e., lignite. Likewise, the use of electricity storage increases compared to the baseline in scenario *Res65-Dem25*, where inflexible decentralized hydrogen supply prevails, but is substituted by centralized hydrogen flexibility in scenario *Res80-Dem25*.

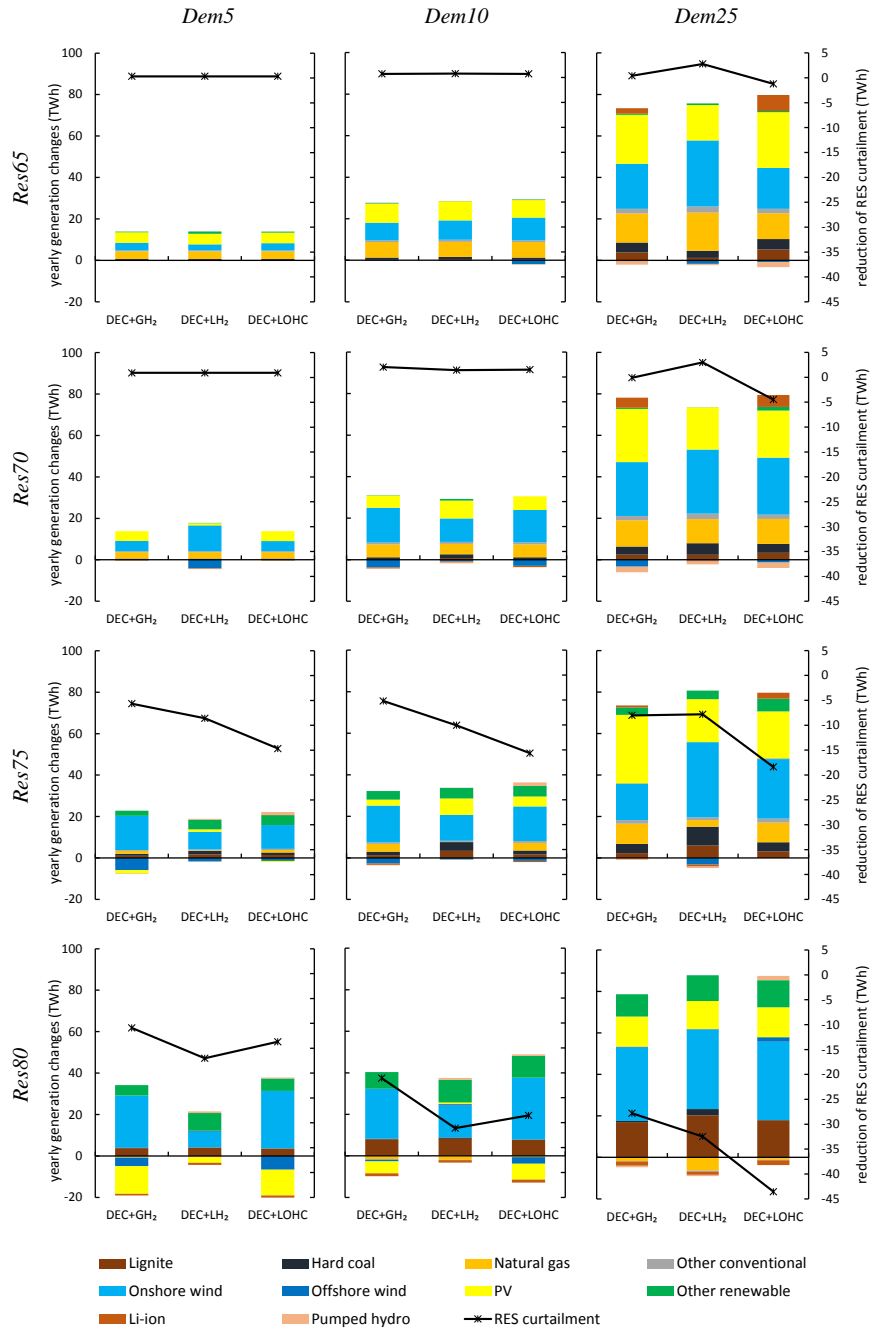
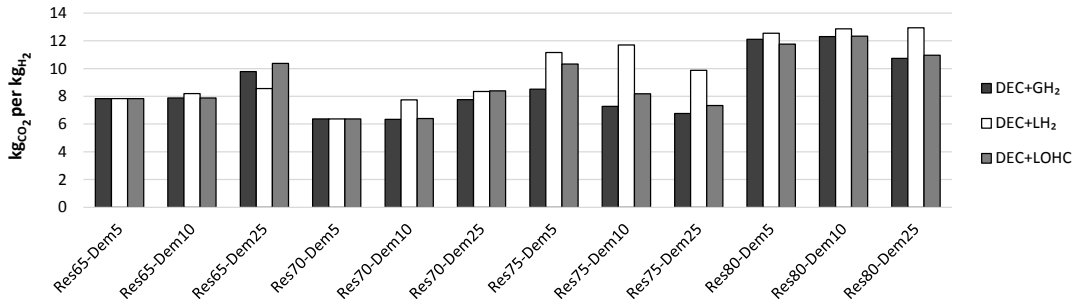


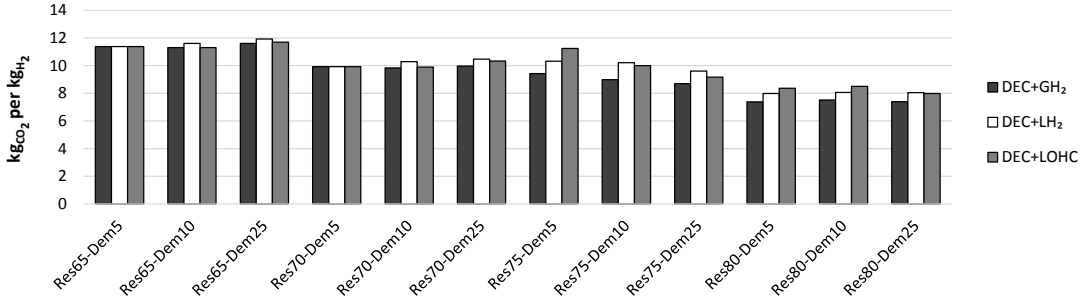
Figure 6: Yearly electricity generation changes compared to the respective base-lines without hydrogen for optimal combinations of decentralized and centralized hydrogen supply chains as shown in Figure 2.

## 2.4 CO<sub>2</sub> emission intensity of hydrogen may not decrease with higher renewable shares

We calculate the CO<sub>2</sub> emission intensity of the hydrogen supplied in two complementary ways (see Section 4.2). The Additional System Emission Intensity of Hydrogen (ASEIH), shown in Figure 7a, takes the full power sector effects of hydrogen provision into account. It is defined as the difference of overall CO<sub>2</sub> emissions between a scenario with hydrogen and the respective baseline without hydrogen, relative to the total hydrogen demand. The ASEIH mirrors the changes in yearly electricity generation induced by hydrogen supply and ranges between 6 and 13 kg CO<sub>2</sub> per kg H<sub>2</sub>.



(a) Additional System Emission Intensity of Hydrogen (ASEIH)



(b) Average Provision Emission Intensity of Hydrogen (APEIH)

Figure 7: Emission metrics

Among the *Res65* scenarios, the emission intensity of hydrogen is higher for high hydrogen demand (*Dem25*) because the greater role of flexible centralized hydrogen supply chains triggers an increase in coal-fired generation. For a renewable share of 70 %, the emission intensity is lower because overall power sector emissions decrease, and the additional hydrogen demand largely integrates renewables without requiring additional fossil generation. In contrast, for high renewable shares of 75 % or 80 %, the ASEIH increases again because the flexibility related to the centralized hydrogen supply chains allows integrating more coal-fired power generation. This is most pronounced for combinations of decentralized electrolysis and LH<sub>2</sub>, as the centralized supply channel has a greater

relevance in overall  $H_2$  supply compared to DEC+GH<sub>2</sub> or DEC+LOHC. Under this metric, thus, the emission intensity of electrolysis-based hydrogen does not necessarily decrease with increasing renewable shares, absent further CO<sub>2</sub> regulation.

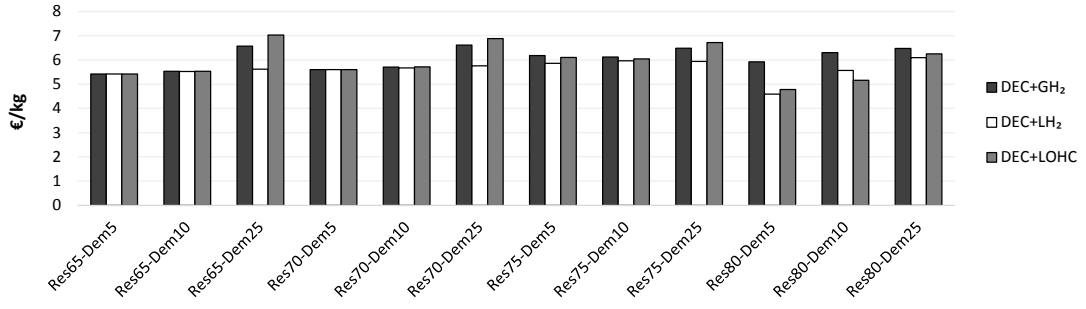
The second metric, Average Provision Emission Intensity of Hydrogen (APEIH), shown in Figure 7b, does not capture the differences to an alternative power sector without hydrogen, but is based on CO<sub>2</sub> emissions prevailing in the hours of actual hydrogen production. The APEIH ranges between 7 and 12 kg CO<sub>2</sub> per kg H<sub>2</sub>. The APEIH is highest for the *Res65* scenarios and generally decreases with increasing renewable shares. It is lowest in supply chains with GH<sub>2</sub>, slightly higher in with LH<sub>2</sub>, and highest for LOHC. This largely reflects the differences in energy efficiency among these options.

For lower renewable shares, the APEIH tends to be higher than the ASEIH; for high renewable shares, the APEIH tends to be lower than the ASEIH. That is, a greater renewable penetration decreases the CO<sub>2</sub> emissions of the electricity mix used to produce hydrogen (APEIH), but additional emissions induced by H<sub>2</sub> do not necessarily decrease (ASEIH). This also indicates that analyses on the emission intensity of (green) hydrogen should generally be interpreted with care.

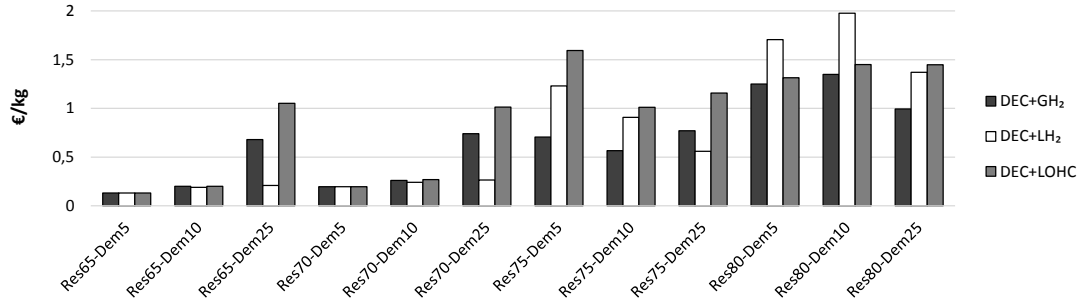
## 2.5 Power sector co-benefits of hydrogen

We illustrate the power sector co-benefits of hydrogen supply in two different ways. First, the Average Provision Costs of Hydrogen (APCH) indicate hydrogen costs from a producer perspective. Over all scenarios, the APCH are between around 5 and 8 €/kg (Figure 8a). These costs are below the current uniform retail price of hydrogen in Germany of around 9.5 €/kg. In general, the APCH increase with hydrogen demand in all scenarios. With increasing shares of renewable energy, the APCH generally increase slightly, with the exception of scenarios *Res80-Dem5* and *Res80-Dem10*. Here, supply chain combinations that include LH<sub>2</sub> or LOHC lead to lower costs because they can make better use of periods with very low electricity prices, which are frequent in this setting.

In contrast to APCH, the Additional System Costs of Hydrogen (ASCH) metric indicates the costs of hydrogen from a power system perspective. ASCH, which are also shown in Figure 2, are smaller than APCH in all scenarios. This difference is substantially more pronounced for higher renewable shares (Figure 8b). The ASCH also include the co-benefits of better renewable energy integration compared to a system without hydrogen. Yet, these benefits cannot be fully internalized by customers at filling stations, as the difference to the more production-oriented APCH metric indicates.



(a) Average Provision Costs of Hydrogen (APCH)



(b) Difference between APCH and ASCH

Figure 8: Average Provision Costs of Hydrogen (APCH) and differences to Additional System Costs of Hydrogen (ASCH).

Second, we illustrate the power sector co-benefits of different hydrogen supply chains with their impacts on the System Costs of Electricity (SCE, Section 4.2). Here, the total co-benefits of integrating the power and hydrogen sectors are attributed to the costs of generating electricity. For renewable shares of 65 % and 70 %, hydrogen hardly has an impact (Figure 9). Yet, SCE decrease markedly for higher renewable shares, up to more than 9 % for a combination of decentralized electrolysis and LOHC in the *Res80-Dem25* scenario. The main driver for these benefits, again, is reduced renewable curtailment.

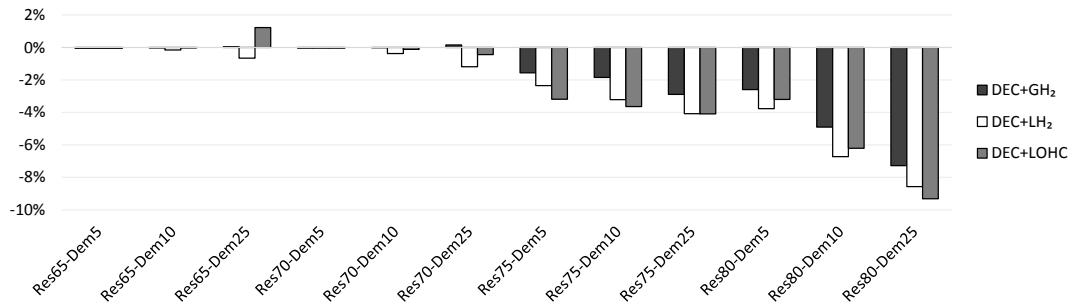


Figure 9: Effect of hydrogen on System Costs of Electricity (SCE)

## 2.6 Sensitivity analyses: impacts of central parameter assumptions on supply chains

Additional model runs show the impact of alternative assumptions for central parameters (see [SI.1](#)).  $\text{GH}_2$  and LOHC tend to improve relative to  $\text{LH}_2$  if the transportation distance decreases, and vice versa, in particular if the share of centralized production is high. If mass hydrogen storage could be placed at filling stations, this would greatly benefit the decentralized supply chain.  $\text{GH}_2$  becomes the dominant option for most scenarios if low-cost cavern storage can be developed.  $\text{LH}_2$  would improve further if boil-off during storage could be avoided. In turn, LOHC would become dominant in most scenarios if free waste heat could be used for dehydrogenation and if existing transportation and storage infrastructure could be used without additional costs.

## 3 Discussion

Our co-optimization of the power and hydrogen sectors highlights the trade-off between energy efficiency and flexibility for different hydrogen supply chains. For lower shares of renewable energy sources and low hydrogen demand, decentralized electrolysis is most beneficial because energy efficiency matters most in such a setting. For higher shares of renewables or higher hydrogen demand, the flexibility benefits of centralized hydrogen options gain importance because these allow to temporally disentangle hydrogen production from demand to make better use of periods with high renewable availability. Among the centralized options,  $\text{LH}_2$  provides the best combination of efficiency, flexibility, and investment cost over the majority of scenarios. Although more energy-efficient,  $\text{GH}_2$  is never part of the cost-minimal solution due to high storage costs. LOHC is largely between  $\text{LH}_2$  and  $\text{GH}_2$ . It offers cheap storage, but also requires substantial amounts of electricity for the relatively inflexible dehydrogenation process at the filling station.

Yet, the Additional System Costs of Hydrogen are relatively similar among optimal supply chain combinations in many scenarios. Thus, real-world investment choices should also take factors into account that the model analysis does not capture. This includes aspects of operational safety and public acceptance, which may favor LOHC, or constraints to renewable energy deployment, which may favor the more energy-efficient options. Sensitivity analyses show how optimal supply chains depend on the (potential) future availability of, e.g., cavern storage or waste heat.

We further show that centralized hydrogen supply chains can deliver relevant power sector co-benefits. Their energy storage capabilities help to make use of lower-cost electricity generation options, in particular renewable surplus generation. Yet, the flexibility that hydrogen provides to the power sector not only facilitates renewable integration, but can also increase the use of conventional generation with low marginal costs. Accordingly, the emission intensity of hydrogen does not necessarily decrease with higher renewable shares, absent further  $\text{CO}_2$  regulation. However, this effect is not specific to hydrogen generation.

It generally occurs when a flexibility resource is added to a power sector with under-utilized emission-intensive generation capacity. This concerns electrical storage [24], electric vehicles [25] and power-to-heat [26].

We conclude that power sector models should represent the flexibility characteristics of hydrogen and other sector coupling strategies in sufficient detail to assess their potential contribution for renewable energy integration. Likewise, system planners and policy makers should properly consider flexibility and efficiency aspects when assessing the role of green hydrogen in future energy transition scenarios. To realize flexibility benefits in actual energy markets, the design of tariffs and taxes should aim for a largely undistorted wholesale price signal along all steps of the hydrogen supply chain [cf. 27], while considering a fair distribution of the co-benefits between hydrogen and electricity consumers.

Future work may address some limitations of this study. Several research design choices we made for clarity and tractability lead to a power sector that is relatively flexibility-constrained. On the demand side, we abstract from a range of potential flexibility sources, such as power-to-heat options or battery-electric vehicles. We also abstract from geographical balancing in the European interconnection. Accordingly, we may overestimate renewable surpluses and, in turn, the benefits of flexible hydrogen supply chains that make use of them. Likewise, we abstract from transmission and distribution grid constraints, which may increase the local value of flexible hydrogen supply. We further do not constrain investments in renewable electricity generation in Germany. A cap on renewable capacity deployment, reflecting public acceptance and planning issues, may increase the relative importance of energy efficiency compared to flexibility. Against this background, future research would be desirable on the efficiency-flexibility trade-off for different hydrogen carriers for long-range bulk transport of green hydrogen from remote areas with very good renewable energy resources, such as Patagonia or Australia. Likewise, extending our analysis to also include the reconversion of hydrogen to electricity in scenarios with full renewable supply would be promising [3, 28].

## 4 Experimental procedures

### 4.1 Model

We use the established open-source power sector model DIETER [26, 29, 30, 31]. For transparency and reproducibility [32], source code, input data, and a complete documentation of the model version used here are available under a permissive open-source license in a public repository [33] (see also [www.diw.de/dieter](http://www.diw.de/dieter)).

The model minimizes the total system costs of providing electricity and hydrogen. The objective function comprises annualized investment costs and hourly variable costs for electricity generation and storage technologies, electrolysis as well as storage, conversion, and transportation of hydrogen. Main model inputs are availability and costs parameters for all technologies as well as hourly time series of electricity demand, hydrogen demand, and renewable capacity factors.



Main decision variables are capacities in the power and hydrogen sectors as well as their hourly use. The optimization is subject to constraints, including market balances for electricity and hydrogen that equate supply and demand in each hour, capacity limits for generation and investment, and a minimum share of renewable energy in electricity supply. The model determines a long-run first-best equilibrium benchmark for a frictionless market. Assuming perfect foresight, DIETER is solved for all consecutive hours of an entire year. Model outputs comprise system costs, optimal capacities and their hourly use, and derived metrics such as emission intensities.

To keep the analysis tractable, the DIETER version used here has no explicit representation of electricity transmission, focuses on Germany only, and abstracts from balancing with the European interconnection. We also do not use some features of the original model, such as demand-side flexibility beyond the hydrogen sector.

The hydrogen sector is modeled with a well-to-tank perspective. It includes one decentralized and three centralized options for providing electrolysis-based hydrogen at filling stations, of which only one can be selected per filling station (Figure 1). Electricity demand along the hydrogen supply chains, that is, for hydrogen production, processing, and distribution facilities, enters the model’s electricity market balance. All costs for hydrogen-related investments enter the model’s objective function. This endogenously captures the use of electricity for different purposes in each hour.

For centralized hydrogen production, we consider alkaline and proton exchange membrane water electrolysis. The hydrogen is either compressed and stored at the production site at up to 250 bar ( $\text{GH}_2$ ), liquefied and stored in insulated tanks ( $\text{LH}_2$ ) or bound to a liquid organic hydrogen carrier (LOHC) in an exothermic hydrogenation reaction and stored in simple tanks. As LOHC, we assume dibenzyltoluene; see [34] for an exposition.  $\text{GH}_2$  and LOHC can be stored without losses;  $\text{LH}_2$  suffers from a boil-off of  $\sim 0.2\%$  per day ( $\sim 52\%$  per year), which lowers its potential for long-term  $\text{H}_2$  storage. For  $\text{GH}_2$ , hydrogen may also be directly prepared for transportation after production, bypassing production site storage. Investments in storage capacity at centralized production sites are unrestricted. Due to minimum filling level requirements, usable storage capacities can be lower than nominal capacities.

For transportation, hydrogen is taken from the respective storage at the centralized production site, re-compressed (if necessary), and transported (time consuming) in special tank trucks to the filling stations.

At filling stations,  $\text{GH}_2$  from centralized electrolysis is either re-compressed and stored at up to 250 bar or directly compressed to 950 bar for the high-pressure buffer storage (bypass option).  $\text{LH}_2$  and LOHC are first stored in unconverted form, where boil-off for  $\text{LH}_2$  is slightly higher at the filling station than at the centralized production site ( $\sim 0.4\%$  per day or  $\sim 77\%$  per year). Spatial limitations and security aspects restrict these storage capacities to two truck loads for all three centralized supply chains.  $\text{LH}_2$  is then cryo-compressed and evaporated, and LOHC dehydrogenated and compressed to be stored in gaseous form at up to 950 bar in high-pressure vessels used as buffer for dispensing. High pressure



storage is limited to 300 kg (one 20 ft container with tubes [35]).

For decentralized hydrogen production, electrolysis is restricted to PEM, which is superior to ALK electrolysis in several dimension relevant for small-scale on-site production, including higher load flexibility [36], lower footprint [36], and easier handling [37]. The hydrogen is immediately compressed and stored at 700-950 bar in high pressure vessels at the filling station. For the high pressure storage and dispensing, the same assumptions apply as for the centralized supply chains.

## 4.2 Cost and emissions metrics

**System Costs of Electricity (SCE)** are the total power sector costs related to overall electricity generation. They include all investment, fixed, and variable power sector costs, but exclude the investment, fixed, and (non-electricity) variable costs of the hydrogen supply chains. Using the SCE, the co-benefits of integrating the power and hydrogen sectors are completely attributed to electricity generation. The SCE treat all electricity generation equally, irrespective of later consumption for conventional electricity demand, demand for hydrogen production and distribution, or losses in the transformation process.

**Additional System Costs of Hydrogen (ASCH)** are defined as the difference in total system costs between a scenario that includes hydrogen and the respective baseline without hydrogen demand, related to total hydrogen supply. The ASCH factor in the total power sector co-benefits of hydrogen supply. ASCH are not directly observable for market participants, but relevant from an energy sector planning perspective.

**Average Provision Costs of Hydrogen (APCH)**, in contrast, sum the annualized costs of the hydrogen infrastructure and yearly electricity costs for hydrogen production, related to total hydrogen supply. Yearly electricity costs are the product of the hourly shadow prices of the model's energy balance and the hourly electricity demand along the hydrogen supply chain, summed up over all hours of a year. The APCH reflect a producer perspective (excluding taxes and fees that are potentially relevant in real-world settings). For alternative leveled costs of hydrogen (LCOH) concepts, see [38].

The **Additional System Emission Intensity of Hydrogen (ASEIH)** relates the overall difference of CO<sub>2</sub> emissions between a scenario with hydrogen and the respective baseline without hydrogen to the total hydrogen supply. Analogously to the ASCH, this metric takes the full power sector effects of hydrogen provision into account. Like ASCH, ASEIH are not directly observable in an actual market, but relevant from an energy sector planning perspective.

The alternative **Average Provision Emission Intensity of Hydrogen (APEIH)** metric is calculated by multiplying hourly average emission intensities of electricity generation with respective hourly electricity consumption for hydrogen supply at all steps of the supply chain (including compression, dehydrogenation etc.), and relating this to overall hydrogen provision. Analogously to the APCH, the APEIH assume a producer perspective.

## 5 Acknowledgments

We thank Markus Reuß and Philipp Runge for fruitful discussions and helpful comments. We are also grateful that Markus Reuß shared a spreadsheet tool to easily calculate electricity demand for compression. We further thank the participants of the following seminars and workshops for valuable feedback: Climate & Energy College at the University of Melbourne, 100 % Renewable Energy workshop at the Australian National University, Strommarkttreffen Berlin, Power-to-X Day at Dechema Frankfurt, and the BB2 research seminar at ifo Munich. We further thank Amine Sehli, Seyed Saeed Hosseinioun, and Justin Werdin for research assistance. Wolf-Peter Schill carried out parts of this work during a research stay at the Energy Transition Hub at the University of Melbourne. We gratefully acknowledge research funding by the German Federal Ministry of Education and Research via the Kopernikus P2X project, research grant 03SFK2B1.

## 6 Author contributions

Conceptualization, W.P.S. and A.Z.; Methodology, F.S., W.P.S., and A.Z.; Software, F.S.; Writing, F.S., W.P.S., and A.Z.; Visualization, F.S. and A.Z.; Project administration and funding acquisition, W.P.S.

## 7 Declaration of interests

The authors declare no competing interests.

## References

- [1] H. de Coninck, A. Revi, M. Babiker, P. Bertoldi, M. Buckeridge, A. Cartwright, W. Dong, J. Ford, S. Fuss, J.-C. Hourcade, D. Ley, R. Mechler, P. Newman, A. Revokatova, S. Schultz, L. Steg, and T. Sugiyama. Strengthening and Implementing the Global Response. In V. Masson-Delmotte, P. Zhai, H.-O. Pörtner, D. Roberts, J. Skea, P. R. Shukla, A. Pirani, W. Moufouma-Okia, C. Péan, R. Pidcock, S. Connors, J. B. R. Matthews, Y. Chen, X. Zhou, M.I. Gomis, E. Lonnoy, T. Maycock, M. Tignor, and T. Waterfield, editors, *Global Warming of 1.5°C. An IPCC Special Report on the Impacts of Global Warming of 1.5°C Above Pre-Industrial Levels and Related Global Greenhouse Gas Emission Pathways, in the Context of Strengthening the Global Response to the Threat of Climate Change, Sustainable Development, and Efforts to Eradicate Poverty*. 2018. Available at: [https://www.ipcc.ch/site/assets/uploads/sites/2/2019/05/SR15\\_Chapter4\\_High\\_Res.pdf](https://www.ipcc.ch/site/assets/uploads/sites/2/2019/05/SR15_Chapter4_High_Res.pdf) [last accessed: Apr. 6, 2020].
- [2] Z. Yan, J. L. Hitt, J. A. Turner, and T. E. Mallouk. Renewable Electricity

- Storage Using Electrolysis. *Proceedings of the National Academy of Sciences*, 2019. [doi:10.1073/pnas.1821686116](https://doi.org/10.1073/pnas.1821686116).
- [3] I. Staffell, D. Scamman, A. Velazquez Abad, P. Balcombe, P. E. Dodds, N. Ekins, P. and Shah, and K. R. Ward. The Role of Hydrogen and Fuel Cells in the Global Energy System. *Energy & Environmental Science*, 12:463–491, 2019. [doi:10.1039/C8EE01157E](https://doi.org/10.1039/C8EE01157E).
  - [4] S. Brynolf, M. Taljegard, M. Grahn, and J. Hansson. Electrofuels for the Transport Sector: A Review of Production Costs. *Renewable and Sustainable Energy Reviews*, 81, Part 2:1887–1905, 2018. [doi:10.1016/j.rser.2017.05.288](https://doi.org/10.1016/j.rser.2017.05.288).
  - [5] P. De Luna, C. Hahn, D. Higgins, S. A. Jaffer, T. F. Jaramillo, and E. H. Sargent. What Would it Take for Renewably Powered Electrosynthesis to Displace Petrochemical Processes? *Science*, 364(6438), 2019. [doi:10.1126/science.aav3506](https://doi.org/10.1126/science.aav3506).
  - [6] M. Z. Jacobson, M. A. Delucchi, Z. A. F. Bauer, C. W. Savannah, E. Chapman, M. A. Cameron, C. Bozonnat, L. Chobadi, H. A. Clonts, P. Enevoldsen, J. R. Erwin, S. N. Fobi, O. K. Goldstrom, E. M. Hennessy, J. Liu, J. Lo, C. B. Meyer, S. B. Morris, K. R. Moy, P. L. O’Neill, I. Petkov, S. Redfern, R. Schucker, M. A. Sontag, J. Wang, E. Weiner, and A. S. Yachanin. 100% Clean and Renewable Wind, Water, and Sunlight All-Sector Energy Roadmaps for 139 Countries of the World. *Joule*, 1(1):108–121, 2017. [doi:10.1016/j.joule.2017.07.005](https://doi.org/10.1016/j.joule.2017.07.005).
  - [7] G. Luderer, Z. Vrontisi, C. Bertram, O. Y. Edelenbosch, R. C. Pietzcker, J. Rogelj, H. S. De Boer, L. Drouet, J. Emmerling, O. Fricko, S. Fujimori, P. Havlík, G. Iyer, K. Keramidas, A. Kitous, M. Pehl, V. Krey, K. Riahi, B. Saveyn, M. Tavoni, D. P. Van Vuuren, and E. Kriegler. Residual Fossil CO<sub>2</sub> Emissions in 1.5-2°C Pathways. *Nature Climate Change*, 8(7):626–633, 2018. [doi:10.1038/s41558-018-0198-6](https://doi.org/10.1038/s41558-018-0198-6).
  - [8] E. S. Hanley, J. P. Deane, and B. P. Ó Gallachóir. The Role of Hydrogen in Low Carbon Energy Futures - A Review of Existing Perspectives. *Renewable and Sustainable Energy Reviews*, 82:3027–3045, 2018. [doi:10.1016/j.rser.2017.10.034](https://doi.org/10.1016/j.rser.2017.10.034).
  - [9] Nature Energy. Editorial: Hydrogen on the Rise. *Nature Energy*, 1, 2016. [doi:10.1038/nenergy.2016.127](https://doi.org/10.1038/nenergy.2016.127).
  - [10] Nature Energy. Editorial: On the Right Track. *Nature Energy*, 4(169), 2019. [doi:10.1038/s41560-019-0366-6](https://doi.org/10.1038/s41560-019-0366-6).
  - [11] C. Breyer, S. Khalili, and D. Bogdanov. Solar Photovoltaic Capacity Demand for a Sustainable Transport Sector to Fulfil the Paris Agreement by 2050. *Progress in Photovoltaics: Research and Applications*, 27(11):978–989, 2019. [doi:10.1002/pip.3114](https://doi.org/10.1002/pip.3114).

- [12] T. Brown, D. Schlachtberger, A. Kies, S. Schramm, and M. Greiner. Synergies of Sector Coupling and Transmission Reinforcement in a Cost-Optimised, Highly Renewable European Energy System. *Energy*, 160:720–739, 2018. [doi:10.1016/j.energy.2018.06.222](https://doi.org/10.1016/j.energy.2018.06.222).
- [13] H. C. Gils and S. Simon. Carbon Neutral Archipelago - 100% Renewable Energy Supply for the Canary Islands. *Applied Energy*, 188:342–355, 2017. [doi:10.1016/j.apenergy.2016.12.023](https://doi.org/10.1016/j.apenergy.2016.12.023).
- [14] D. L. de Tena and T. Pregger. Impact of Electric Vehicles on a Future Renewable Energy-Based Power System in Europe with a Focus on Germany. *International Journal of Energy Research*, 42(8):2670–2685, 2018. [doi:10.1002/er.4056](https://doi.org/10.1002/er.4056).
- [15] J. Michalski, U. Büngrer, F. Crostogino, S. Donadei, G.-S. Schneider, T. Pregger, K.-K. Cao, and D. Heide. Hydrogen Generation by Electrolysis and Storage in Salt Caverns: Potentials, Economics and Systems Aspects with Regard to the German Energy Transition. *International Journal of Hydrogen Energy*, 42(19):13427–13443, 2017. [doi:10.1016/j.ijhydene.2017.02.102](https://doi.org/10.1016/j.ijhydene.2017.02.102).
- [16] B. Emonts, M. Reuß, P. Stenzel, L. Welder, F. Knicker, T. Grube, K. Görner, M. Robinius, and D. Stolten. Flexible Sector Coupling with Hydrogen: A Climate-Friendly Fuel Supply for Road Transport. *International Journal of Hydrogen Energy*, 44(26):12918–12930, 2019. [doi:10.1016/j.ijhydene.2019.03.183](https://doi.org/10.1016/j.ijhydene.2019.03.183).
- [17] G. Glenk and S. Reichelstein. Economics of Converting Renewable Power to Hydrogen. *Nature Energy*, 4(3):216–222, 2019. [doi:10.1038/s41560-019-0326-1](https://doi.org/10.1038/s41560-019-0326-1).
- [18] P. Kluschke and F. Neumann. Interaction of a Hydrogen Refueling Station Network for Heavy-Duty Vehicles and the Power System in Germany for 2050, 2019. Available at: <https://arxiv.org/ftp/arxiv/papers/1908/1908.10119.pdf>.
- [19] M. Reuß, T. Grube, M. Robinius, P. Preuster, P. Wasserscheid, and D. Stolten. Seasonal Storage and Alternative Carriers: A Flexible Hydrogen Supply Chain Model. *Applied Energy*, 200:290–302, 2017. [doi:10.1016/j.apenergy.2017.05.050](https://doi.org/10.1016/j.apenergy.2017.05.050).
- [20] P. Runge, C. Sölch, J. Albert, P. Wasserscheid, G. Zöttl, and V. Grimm. Economic Comparison of Different Electric Fuels for Energy Scenarios in 2035. *Applied Energy*, 233-234:1078–1093, 2019. [doi:10.1016/j.apenergy.2018.10.023](https://doi.org/10.1016/j.apenergy.2018.10.023).
- [21] L. Welder, D. S. Ryberg, L. Kotzur, T. Grube, M. Robinius, and D. Stolten. Spatio-Temporal Optimization of a Future Energy System for Power-to-Hydrogen Applications in Germany. *Energy*, 158:1130–1149, 2018. [doi:10.1016/j.energy.2018.05.059](https://doi.org/10.1016/j.energy.2018.05.059).

- [22] C. Yang and J. Ogden. Determining the Lowest-Cost Hydrogen Delivery Mode. *International Journal of Hydrogen Energy*, 32(2):268–286, 2007. [doi:10.1016/j.ijhydene.2006.05.009](https://doi.org/10.1016/j.ijhydene.2006.05.009).
- [23] P. Preuster, C. Papp, and P. Wasserscheid. Liquid Organic Hydrogen Carriers (LOHCs): Toward a Hydrogen-Free Hydrogen Economy. *Accounts of Chemical Research*, 50(1):74–85, 2017. [doi:10.1021/acs.accounts.6b00474](https://doi.org/10.1021/acs.accounts.6b00474).
- [24] J. Egerer and W.-P. Schill. Power System Transformation Toward Renewables: Investment Scenarios for Germany. *Economics of Energy & Environmental Policy*, 3(2):29–43, 2014. [doi:10.5547/2160-5890.3.2.jege](https://doi.org/10.5547/2160-5890.3.2.jege).
- [25] W.-P. Schill and C. Gerbaulet. Power System Impacts of Electric Vehicles in Germany: Charging with Coal or Renewables? *Applied Energy*, 156:185–196, 2015. [doi:10.1016/j.apenergy.2015.07.012](https://doi.org/10.1016/j.apenergy.2015.07.012).
- [26] W.-P. Schill and A. Zerrahn. Flexible Electricity Use for Heating in Markets with Renewable Energy. *Applied Energy*, 266, 2020. [doi:10.1016/j.apenergy.2020.114571](https://doi.org/10.1016/j.apenergy.2020.114571).
- [27] O. J. Guerra, J. Eichman, J. Kurtz, and B.-M. Hodge. Cost Competitiveness of Electrolytic Hydrogen. *Joule*, 3(10):2425–2443, 2019. [doi:10.1016/j.joule.2019.07.006](https://doi.org/10.1016/j.joule.2019.07.006).
- [28] L. Welder, P. Stenzel, N. Ebersbach, P. Markewitz, M. Robinius, B. Emonts, and D. Stolten. Design and Evaluation of Hydrogen Electricity Reconversion Pathways in National Energy Systems Using Spatially and Temporally Resolved Energy System Optimization. *International Journal of Hydrogen Energy*, 44(19):9594–9607, 2019. [doi:10.1016/j.ijhydene.2018.11.194](https://doi.org/10.1016/j.ijhydene.2018.11.194).
- [29] A. Zerrahn and W.-P. Schill. Long-Run Power Storage Requirements for High Shares of Renewables: Review and a New Model. *Renewable and Sustainable Energy Reviews*, 79:1518–1534, 2017. [doi:10.1016/j.rser.2016.11.098](https://doi.org/10.1016/j.rser.2016.11.098).
- [30] W.-P. Schill, A. Zerrahn, and F. Kunz. Prosumage of Solar Electricity: Pros, Cons, and the System Perspective. *Economics of Energy & Environmental Policy*, 6(1):7–31, 2017. [doi:10.5547/2160-5890.6.1.wsch](https://doi.org/10.5547/2160-5890.6.1.wsch).
- [31] W.-P. Schill and A. Zerrahn. Long-Run Power Storage Requirements for High Shares of Renewables: Results and Sensitivities. *Renewable and Sustainable Energy Reviews*, 83:156–171, 2018. [doi:10.1016/j.rser.2017.05.205](https://doi.org/10.1016/j.rser.2017.05.205).
- [32] S. Pfenninger. Energy Scientists Must Show Their Workings. *Nature*, 542(393), 2017. [doi:10.1038/542393a](https://doi.org/10.1038/542393a).
- [33] A. Zerrahn, W.-P. Schill, and F. Stöckl. DIETER Model Version for the Paper “Optimal Hydrogen Supply Chains: Co-Benefits for Integrating Renewable Energy Sources”. Zenodo, 2020. [doi:10.5281/zenodo.3693306](https://doi.org/10.5281/zenodo.3693306).

- [34] M. Eypasch, M. Schimpe, A. Kanwar, T. Hartmann, S. Herzog, T. Frank, and T. Hamacher. Model-Based Techno-Economic Evaluation of an Electricity Storage System Based on Liquid Organic Hydrogen Carriers. *Applied Energy*, 185:320–330, 2017. [doi:10.1016/j.apenergy.2016.10.068](https://doi.org/10.1016/j.apenergy.2016.10.068).
- [35] Hexagon Composites. Presentation of Hexagon Composites, 2016. Available at: <https://www.h2fc-fair.com/hm16/images/forum/pdf/02tuesday/1300.pdf> [last accessed: Apr. 6, 2020].
- [36] C. Mittelsteadt, T. Norman, M. Rich, and J. Willey. *PEM Electrolyzers and PEM Regenerative Fuel Cells Industrial View*, chapter 11, pages 159–181. Elsevier, Amsterdam, 2015.
- [37] Linde. Wasserstoff als Energieträger & Kraftstoff, 2016. Available at: [https://www.solarinitiativen.de/wp-content/uploads/1\\_fr\\_02\\_stiller\\_wasserstoff.pdf](https://www.solarinitiativen.de/wp-content/uploads/1_fr_02_stiller_wasserstoff.pdf) [last accessed: Apr. 6, 2020].
- [38] W. Kuckshinrichs and J. C. Koj. Levelized Cost of Energy from Private and Social Perspectives: The Case of Improved Alkaline Water Electrolysis. *Journal of Cleaner Production*, 203:619–632, 2018. [doi:10.1016/j.jclepro.2018.08.232](https://doi.org/10.1016/j.jclepro.2018.08.232).

## SI Supplemental Information

### SI.1 Sensitivities

We carry out a range of sensitivity calculations to explore how key parameter assumptions affect numerical model results. Specifically, we investigate the effects of varying transportation distances, alternatively assume that mass storage for decentralized hydrogen supply is available, alternatively assume that low-cost cavern storage for  $\text{GH}_2$  is available as well as  $\text{LH}_2$  storage without boil-off, and examine cost-free heat supply as well as cost-free transportation and storage infrastructure for LOHC.

### SI.1.1 Transportation distance

Alternatively to the baseline assumption of a 500 km overall transportation distance for centrally produced hydrogen, we examine the effects of 200 and 800 km transportation distances. In general, a shorter/longer transportation distance increases/decreases the shares of centralized hydrogen supply chains in the optimal solution, see Figures [SI.1](#) and [SI.2](#). Moreover, with a shorter transportation distance, centralized technologies are now part of the optimal technology portfolio in some scenarios, while for a longer transportation distance, centralized supply chains drop out in some scenarios.

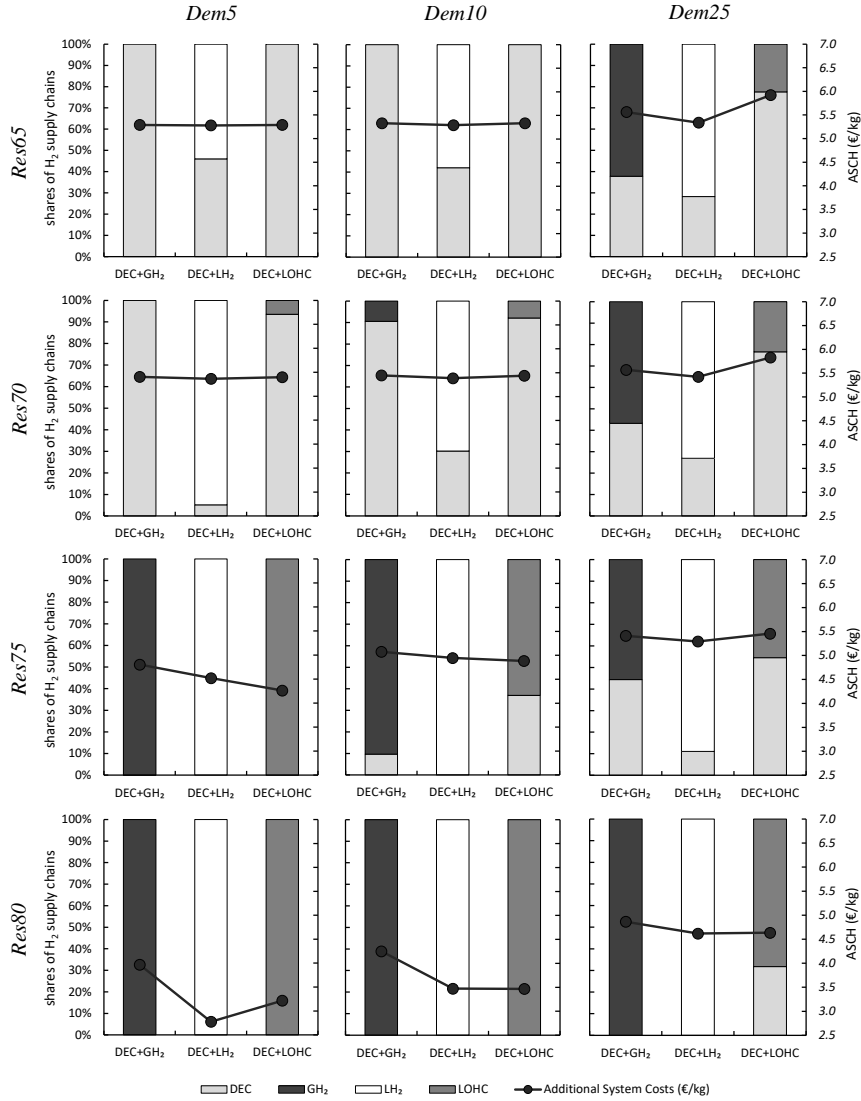


Figure SI.1: Optimal combinations of decentralized and centralized hydrogen supply chains and Additional System Costs of Hydrogen (ASCH) for different scenarios - sensitivity with 200 km overall transportation distance.



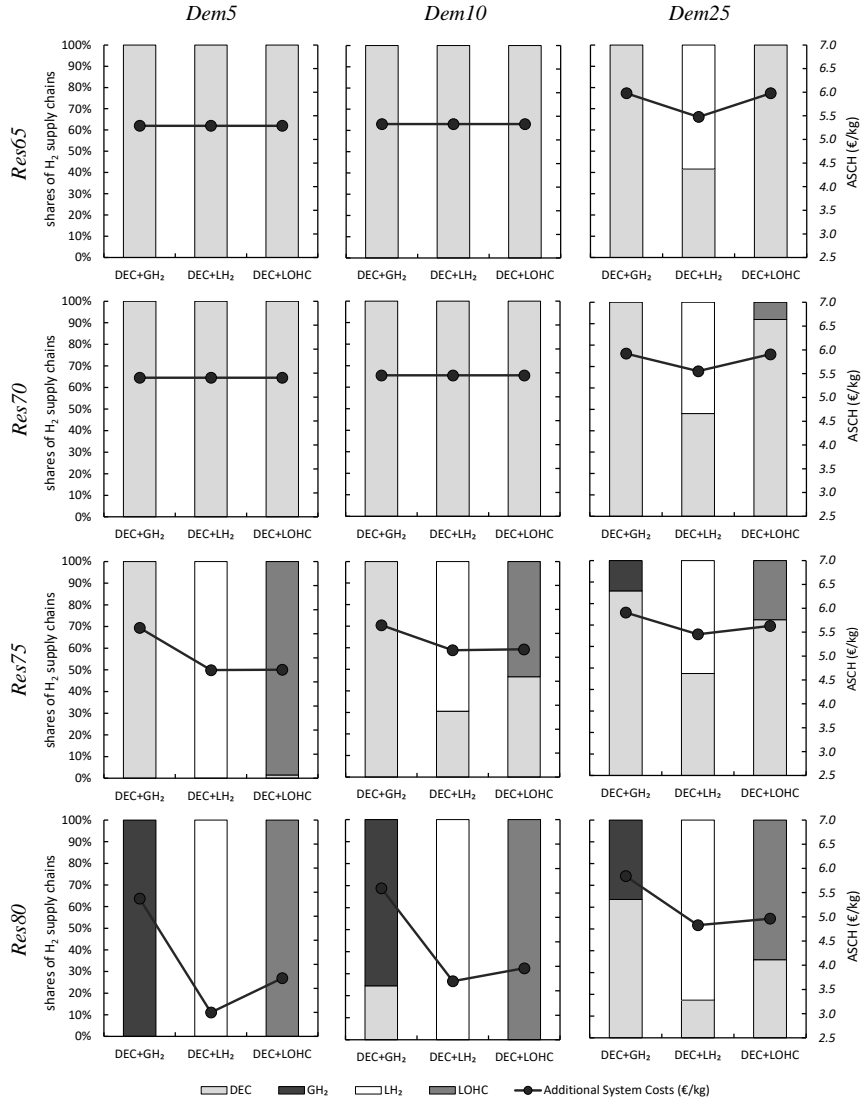


Figure SI.2: Optimal combinations of decentralized and centralized hydrogen supply chains and Additional System Costs of Hydrogen (ASCH) for different scenarios - sensitivity with 800 km overall transportation distance.

In general, a longer/shorter transportation distance increases/decreases the overall costs of the centralized hydrogen supply chain. The spread in costs across supply chain combinations within scenarios tends to increase with transportation distance. Yet, the overall least-cost options are robust, with  $\text{LH}_2$  as dominant centralized supply chain in the optimal solution. Cost outcomes are fairly robust with respect to the transportation distance because the share of transportation-related costs in the overall costs of hydrogen provision are relatively small.

In more detail, a change in the the average transportation distance has two effects on the costs of hydrogen supply. First, variable transportation costs (fuel and driver wage) are proportional to the transportation distance. For the sensitivity calculations with 800 km and 200 km overall transportation distance, the

variable costs increase/decrease by 60 %. While the relative effect is the same for all three centralized supply chains, the effect on absolute cost is highest for  $\text{GH}_2$  and also more pronounced for LOHC than for  $\text{LH}_2$ , see Figure SI.3a.

Second, longer/shorter distances imply that each truck-trailer combination is occupied for a longer/shorter time period. Consequently, the fleet capacity needs to be increased or can be reduced, respectively. Figure SI.3b shows transportation capacity investment costs per kg of hydrogen supplied through a specific supply chain averaged over all *Res-Dem*-scenarios. The pattern is identical to the one for variable costs, yet with less impact in absolute terms.

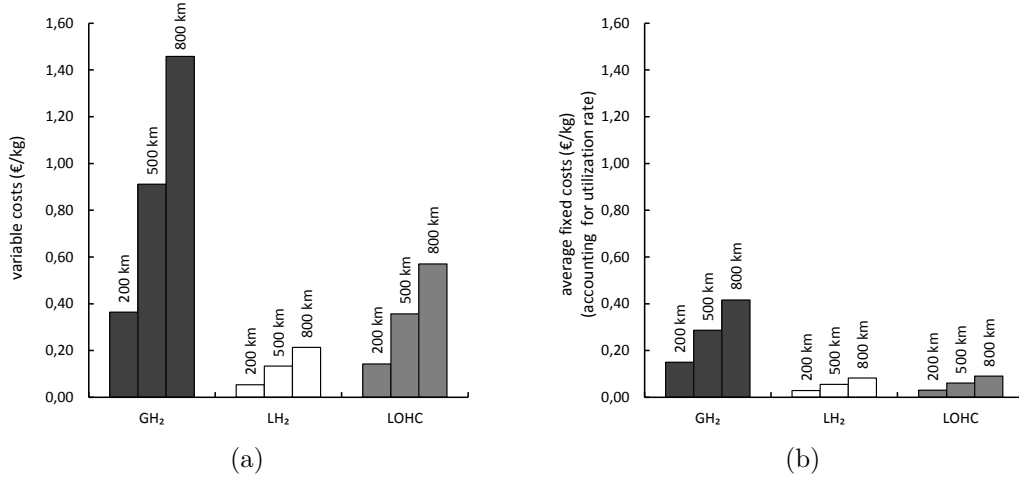


Figure SI.3: Average transportation capacity investment costs and variable costs per kg of hydrogen supplied through the respective channel

## SI.1.2 Mass storage for decentralized hydrogen supply

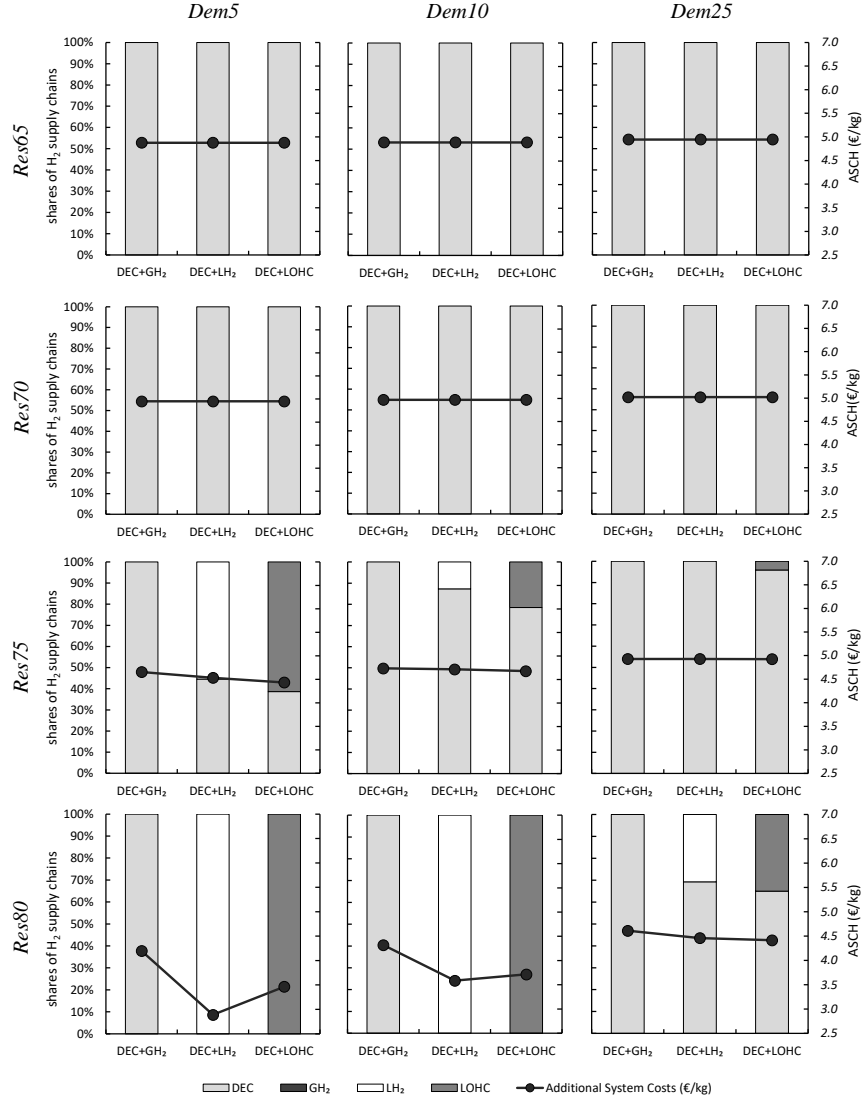


Figure SI.4: Optimal combinations of decentralized and centralized hydrogen supply chains and Additional System Costs of Hydrogen (ASCH) for different scenarios - sensitivity with mass storage available for decentralized production.

Under baseline assumptions, mass hydrogen storage is not available at filling stations for decentralized supply because of space requirements and security concerns. Alternatively, we assume that relatively cheap mass storage at 250 bar can be deployed at filling stations, with the same techno-economic assumptions as for centralized GH<sub>2</sub> storage. Table [SI.13](#) gives an overview of the necessary changes with respect to compression processes and storage infrastructure.

As a consequence, decentralized production of hydrogen becomes more temporally flexible and loses its major disadvantage compared to centralized pro-

duction. Given that decentralized hydrogen supply is more energy-efficient, its share substantially increases for most supply-chain combinations and *Res-Dem*-scenarios (Figure [SI.4](#)), except for the ones with the highest renewable surpluses, i.e., *Res80-Dem5* and *Res80-Dem10*, where all demand is still supplied by centralized technologies. Here, centralized production of  $\text{LH}_2$  and LOHC still profits from a larger optimal storage size and the according flexibility. Centrally produced  $\text{GH}_2$  drops out completely. As expected, with the additional flexibility option, the ASCH decrease slightly and the spread in costs between different supply chain combinations within each scenario rather decreases. Finally, the pattern of least-cost options across scenarios is robust, except for scenarios *Res75-Dem25* and *Res80-Dem25* where the cost-optimal technology portfolio now contains LOHC rather than  $\text{LH}_2$ .

### SI.1.3 Cavern storage for GH<sub>2</sub>

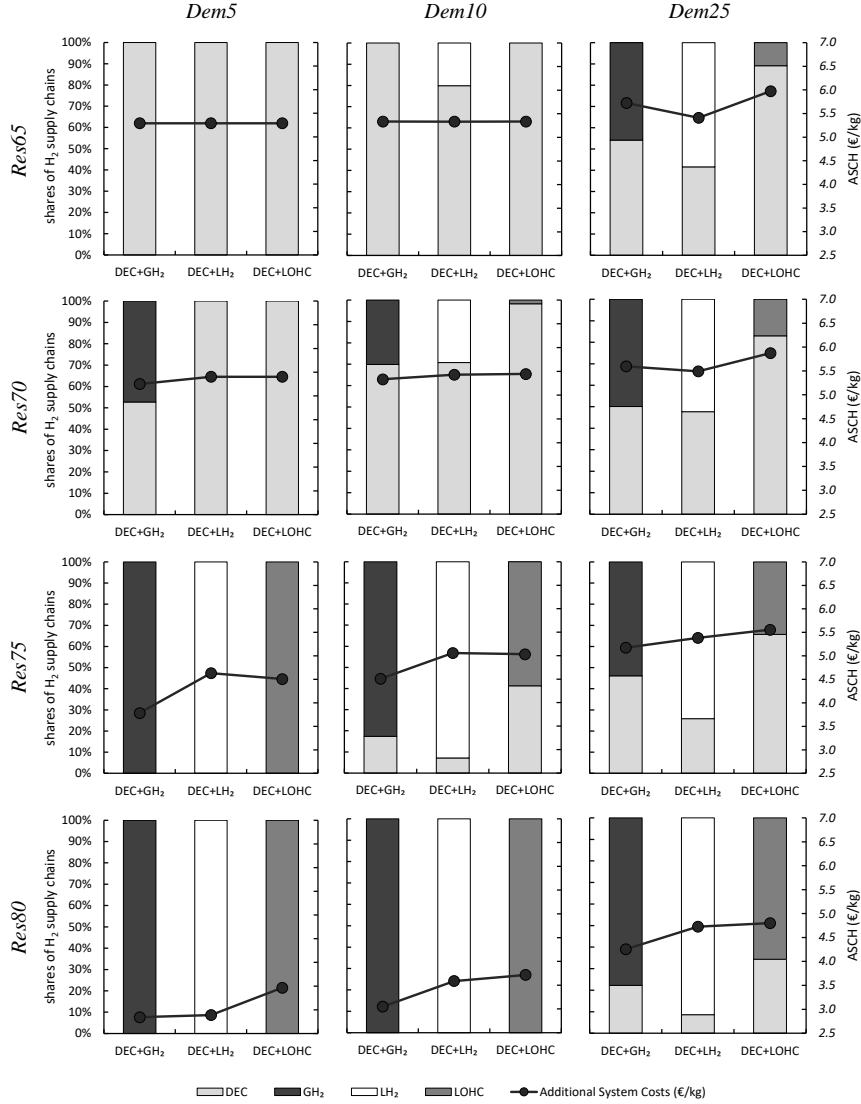


Figure SI.5: Optimal combinations of decentralized and centralized hydrogen supply chains and Additional System Costs of Hydrogen (ASCH) for different scenarios - sensitivity with cavern storage available for centralized GH<sub>2</sub> production.

Low-cost cavern storage would provide flexibility for centralized GH<sub>2</sub> production at very low costs of 3.5 €/kg, which is about one third of the costs of LOHC or LH<sub>2</sub> storage. Tables [SI.4](#) and [SI.6](#) list the altered requirements for compression processes.

If cavern storage is available, the share of centralized GH<sub>2</sub> production increases substantially for all scenarios, see Figure [SI.5](#). In contrast to the results under default assumptions, the ASCH of the supply chain (DEC+)GH<sub>2</sub> are now

lower than for the other options in most scenarios, especially if the share of renewable energy sources is high or H<sub>2</sub> demand is low. Moreover, Figure [SI.6](#) illustrates that the use of cavern storage exhibits a seasonal pattern, as prevalent for LOHC in the baseline specification, yet with higher storage capacity due to low investment costs. Accordingly, the (non-)availability of cavern storage is a relevant driver of numerical model results.

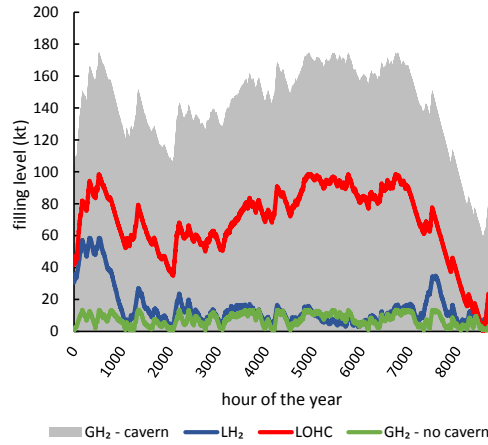


Figure SI.6: Temporal storage use patterns also including cavern storage for scenario *Res80-Dem25*

### SI.1.4 No boil-off for LH<sub>2</sub>

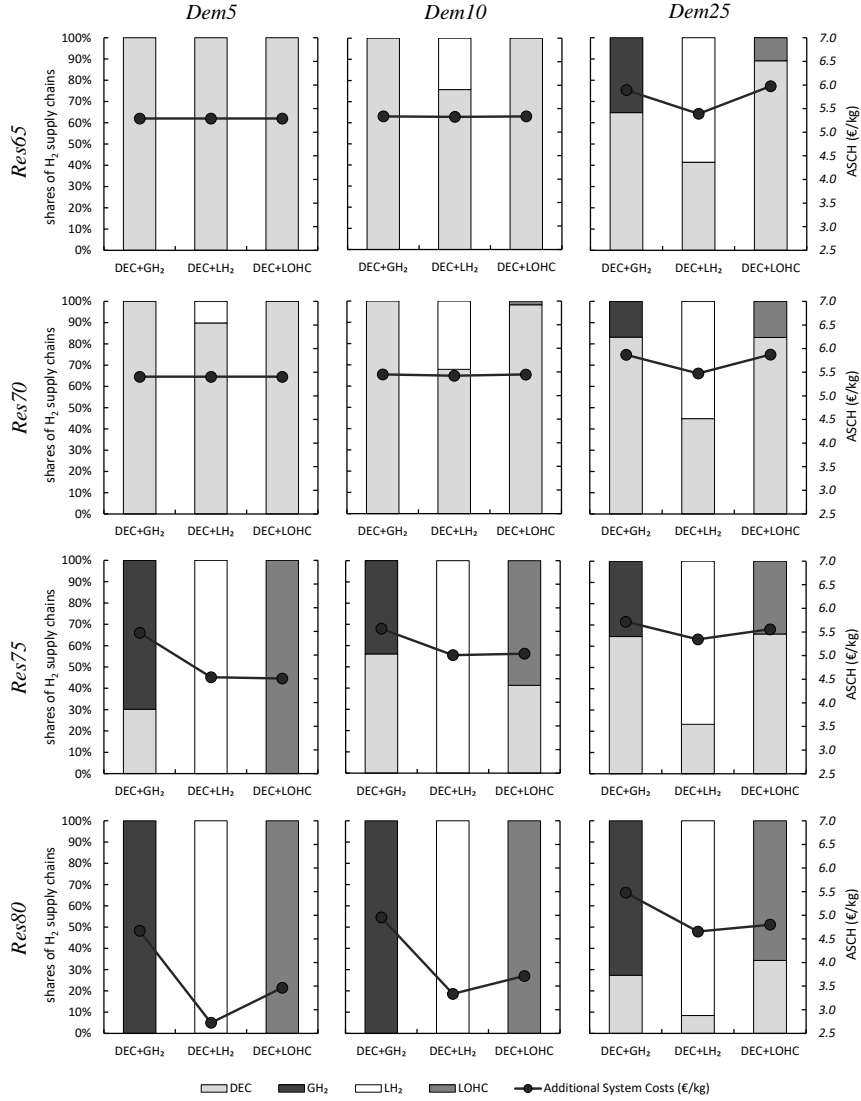


Figure SI.7: Optimal combinations of decentralized and centralized hydrogen supply chains and Additional System Costs of Hydrogen (ASCH) for different scenarios - sensitivity with no boil-off for LH<sub>2</sub> storage.

We assess the effects of LH<sub>2</sub> boil-off during storage and transportation by counter-factually setting it to zero. Figure [SI.7](#) shows the results. The optimal shares of LH<sub>2</sub> compared to decentralized hydrogen production slightly increase in some cases, but effects are small. The average increase is 3.2 percentage points, and the largest increase is 10.2 percentage points in scenario *Res70-Dem5*. Likewise, the effect on H<sub>2</sub> costs is small, with an average cost reduction of 1.8 % and a maximum decrease of 7.0 % in scenario *Res80-Dem10*. The pattern of least-cost

options is robust with the combination containing  $\text{LH}_2$  now additionally optimal for *Res75-Dem10*.

While the effect on costs and optimal technology shares is limited,  $\text{LH}_2$  without boil-off is better suited as long-term or seasonal storage. Its use pattern changes substantially and resembles that of LOHC under default assumptions. Figure SI.8 exemplarily illustrates this point for scenario *Res80-Dem25*.

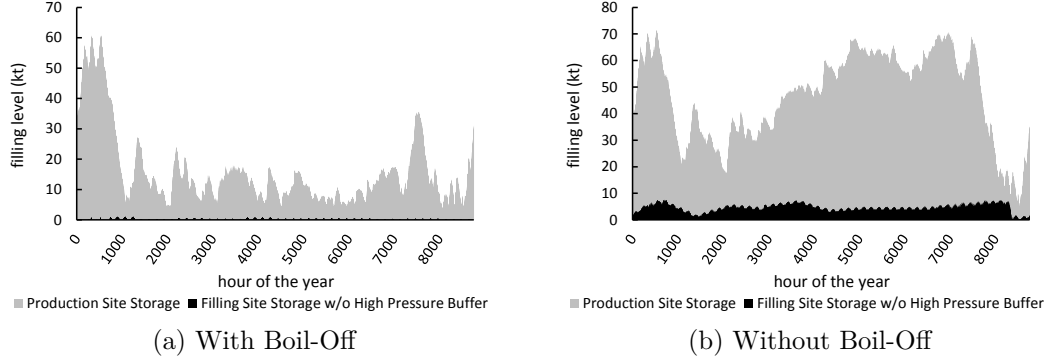


Figure SI.8: Temporal storage use patterns of  $\text{LH}_2$  mass storage at the production site for scenario *Res80-Dem25*

Additionally, we find that  $\text{LH}_2$  storage at the filling station becomes relatively more important if there is no boil-off. Under default assumptions, boil-off at the filling station was slightly higher than at the production site. Without boil-off, the two storage options are identical in terms of losses over time. Thus, the division of storage between the production and filling sites allows for a more efficient use of transportation capacities. This results in a decrease of transportation infrastructure costs of 5.5 % per kg of hydrogen in the scenario *Res80-Dem25*.



### SI.1.5 Free heat supply for LOHC dehydrogenation

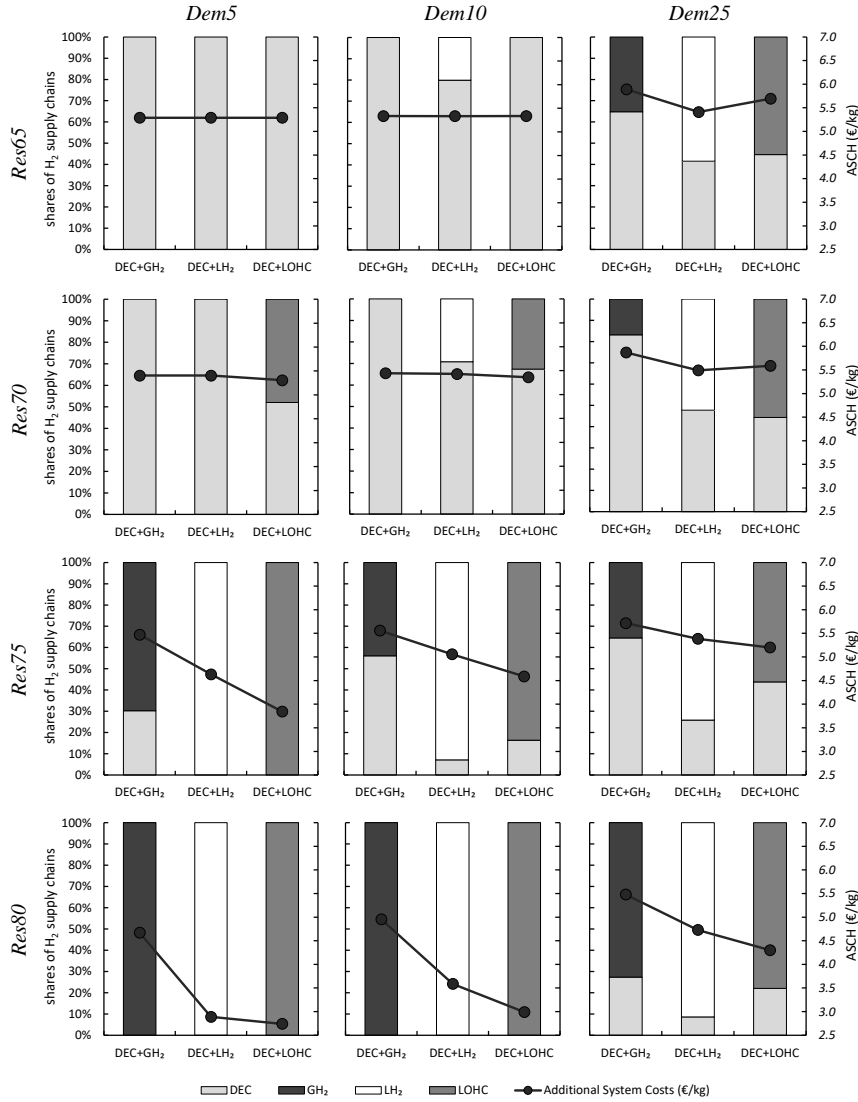


Figure SI.9: Optimal combinations of decentralized and centralized hydrogen supply chains and Additional System Costs of Hydrogen (ASCH) for different scenarios - sensitivity with free heat supply for dehydrogenation.

LOHC has a relatively high electricity demand for dehydrogenation, which is additionally temporally inflexible, that may hold back its extended use. We carry out a sensitivity calculation where the required heat is available free of costs, for instance, because industrial waste heat is available. Figure SI.9 shows the results. Compared to default assumptions, the share of LOHC increases in most scenarios. Also the ASCH for combinations of decentralized electrolysis and LOHC decrease. With free heat supply, the LOHC supply chain is the least-cost solution for all scenarios with renewable shares of 75 % or 80 %.

### SI.1.6 Free transportation and production site storage infrastructure for LOHC

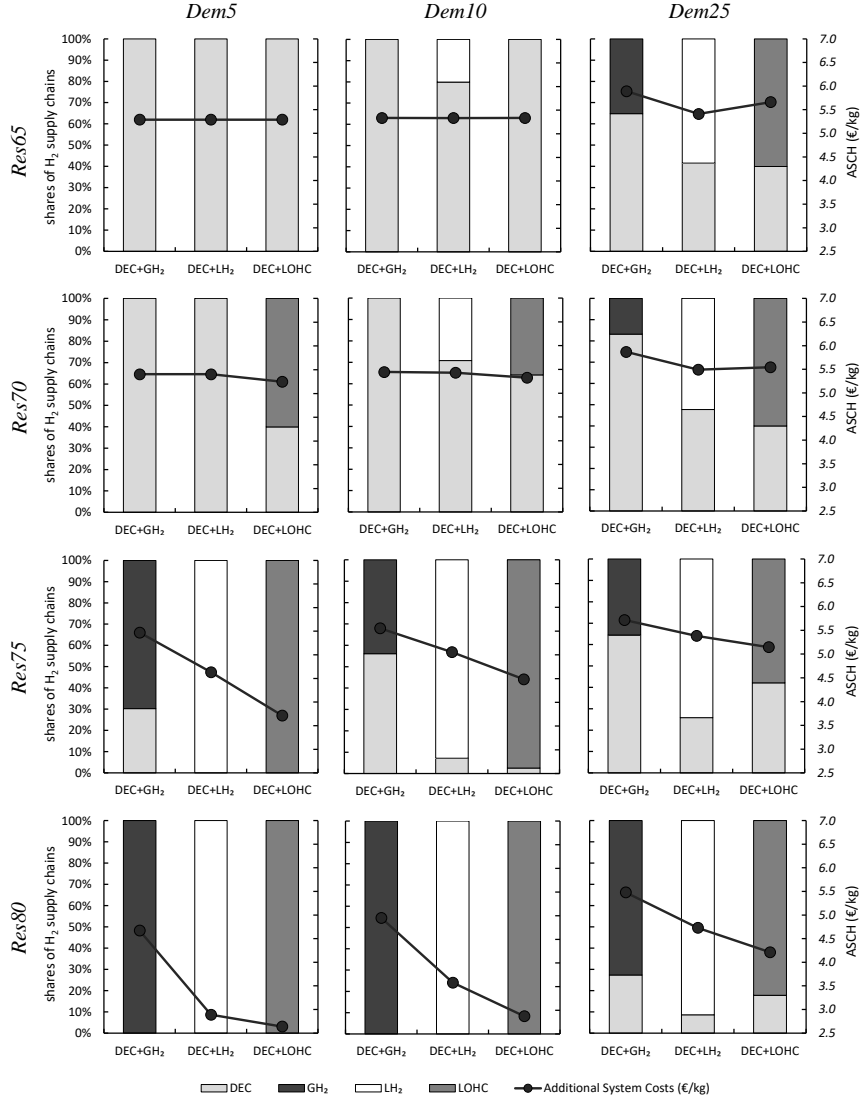


Figure SI.10: Optimal combinations of decentralized and centralized hydrogen supply chains and Additional System Costs of Hydrogen (ASCH) for different scenarios - sensitivity with free infrastructure for LOHC storage and transportation.

Proponents of LOHC argue that existing infrastructure may be used for the LOHC supply chain, especially storage at the production site and filling stations as well as transportation facilities [1]. To address this point in a sensitivity calculation, we assume that storage and transportation capacities do not incur additional costs. Note that the expected lifetime of trucks is 12 years. The cost

advantage of free transportation capacities would at most last for this time period. The results in Figure [SL.10](#) show that the optimal share of LOHC increases only moderately in many scenarios. In contrast, the ASCH decrease substantially for all supply chains containing LOHC. As for the sensitivity calculation with free heat supply for dehydrogenation, the supply chain involving LOHC is the least-cost option in the scenarios with high renewable penetration also in this case (75 % or 80 %).

## SI.2 Key power sector data

We apply our model to 2030 scenarios for Germany. To embed the analysis in a plausible mid-term future setting, electricity generation and storage capacities lean on the medium scenario B of the Grid Development Plan 2019 (*Netzentwicklungsplan*, NEP [2]), an official projection of the German electricity market, which transmission system operators base their investments on.

NEP capacities for wind power, both onshore and offshore, solar PV, and battery storage serve as lower bounds for investments. NEP capacities for fossil plants, biomass plants, and run-of-river hydro power serve as upper bounds, where natural gas capacities are split evenly between combined- and open-cycle gas turbines. Coal capacities are largely in line with current German coal phase-out plans that target at most 9 and 8 GW lignite and hard coal by 2030, respectively. Investments for pumped storage are bounded from below by today's value and from above by the NEP value. Figure SI.11 summarizes the capacity bounds for the power sector.

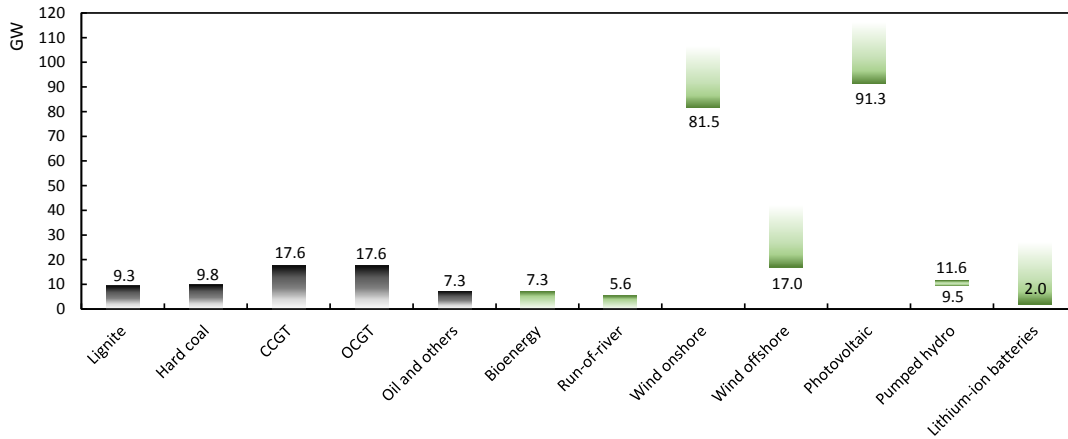


Figure SI.11: Lower and upper bounds for capacity investments in the power sector

Cost and technical parameters for power plants [3] and storage [4, 5] are based on established medium-term projections. Fuel costs and the CO<sub>2</sub> price of 29.4 €/t follow the middle NEP scenario B 2030. The hourly electricity load is representative for an average year and is taken from the Ten-Year Network Development Plan 2030 of the European Network of Transmission System Operators for Electricity [6]. Annual load sums up to around 550 Terawatt hours (TWh). Time series of hourly capacity factors for wind and PV are based on re-analysis data of the average weather year 2012 [7, 8].

All input data is available in a spreadsheet provided together with the open-source model [9].

## SI.3 Key hydrogen sector data

In the following, we present key assumptions on hydrogen sector parameters and fuel demand that are central drivers of the results. Full account of all input data is given in [SI.3.3](#).

### SI.3.1 H<sub>2</sub> infrastructure

PEM electrolysis is six percentage points more efficient than the ALK technology (71 % versus 66 %), but has about one-third higher specific investment costs (905 €/kW<sub>el</sub> versus 688 €/kW<sub>el</sub>). Moreover, based on industry data [\[10\]](#), we assume that investment costs of centralized electrolysis are 20 % lower than those of decentralized production.

Cost differences also exist for hydrogen transportation. Trailers for GH<sub>2</sub> require high pressure tubes (764 €/kg), for LH<sub>2</sub> an insulated tank (190 €/kg), and for LOHC only a simple standard tank (93 €/kg). Differences in variable costs are determined by the net loading capacity per truck, where GH<sub>2</sub> is most expensive with 0.91 €/kg, compared to 0.36 €/kg and 0.13 €/kg for LOHC and LH<sub>2</sub>, respectively. Fuel consumption (Diesel), wages for drivers, and (un-)loading times are assumed to be identical across all supply chains.

Investment costs for hydrogen storage are the central parameter that determines whether flexibility of a supply chain is economical. The costs of GH<sub>2</sub> storage at 250 bar (459 €/kg) is substantially higher than for LH<sub>2</sub> (14 €/kg) and LOHC (10 €/kg). LOHC has a degradation rate of 0.1 % per supply-cycle, entailing additional costs of 0.6 €/kg. We interpret these cost as LOHC rental rate. High-pressure gaseous (buffer) storage at the filling station is more expensive (612 €/kg) and requires a high minimum filling level in order to ensure pressure above 700 bar for dispensing. This reduces the effective available storage capacity further.

The techno-economic characteristics of the four hydrogen supply chains entail an efficiency-flexibility trade-off with respect to their electricity demand. Decentralized production is relatively energy-efficient, but needs to be almost on-time due to a lack of cheap storage options. The three centralized supply chains are less efficient, but (partly) provide cheap storage options that allow to shift energy intensive electrolysis to hours with high (renewable) electricity supply. Electricity demand for the remaining, inflexible processes to prepare stored hydrogen for dispensing at the filling station (recompression, cryo-compression, and evaporation or dehydrogenation), is comparably low. Figure [SI.12](#) contrasts overall electricity demand with largely inflexible (i.e., non-shiftable) electricity demand at the filling station for different hydrogen supply chains across all scenarios. Within-channel deviations (min & max) are due to the choice of electrolysis technology and losses during storage.

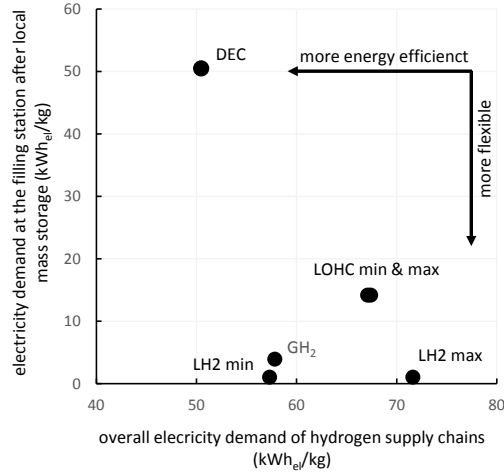


Figure SI.12: The (realized) efficiency-flexibility trade-off for different hydrogen supply chains across all scenarios.

### SI.3.2 H<sub>2</sub> demand

H<sub>2</sub> demand for private and public road-based passenger transportation in Germany leans on a forecast for the year 2030 [11]. To convert gasoline and diesel consumption to H<sub>2</sub> demand [12], shares of fuel consumption for 2030 are assumed to be identical to those in 2017 [13]. Table SI.1 shows the resulting demands for the scenarios where 5 %, 10 % or 25 % of private and public road-based passenger traffic in Germany in 2030 is fueled by hydrogen.

The hourly H<sub>2</sub> demand profile at the filling stations is assumed to be identical to today's for gasoline and diesel fuel. As data for Germany is not available, we resort to U.S. data for hourly and weekly [14] as well as for monthly [15] demand characteristics. Moreover, each filling station dispenses at most 1000 kg hydrogen per day [16]. This results in 976, 1952, and 4880 filling stations for the 5, 10, and 25 % demand scenarios, respectively.

Table SI.1: Traffic Data (2030 projection)

Scenario	H <sub>2</sub> demand	
	TWh	kt
5 %	9.053	271.610
10 %	18.160	543.220
25 %	45.265	1,358.050

Finally, depending on the average loading capacity and time a car spends at the filling station, a small amount needs to be added to the average costs of

hydrogen to cover dispenser costs (around 0.1 € for 5 kg per car with an average filling time of 7 min and a filling station capacity of 1000 kg/d, compare [17]). These costs are identical across all supply chain combinations and, thus, have no effect on their ranking.

### SI.3.3 Data tables

In the following, we list all data and sources for techno-economic parameters concerning the H<sub>2</sub> infrastructure. As parameter projections for 2030 are scarce except for electrolysis, we resort to values for currently existing or planned sites. All cost parameters are stated in euros (€). For conversion from U.S. dollar (\$), we assume an exchange rate of one. As the literature on cost parameters does often not provide information on the reference year, we refrain from correcting for inflation. Unless stated otherwise, kg is always short for kg<sub>H<sub>2</sub></sub>. To calculate electricity demand for compression and scale investment costs, we follow [18]. Pursuing a conservative approach, we always calculate energy demand for hydrogen compression for the least favorable initial pressure conditions. All data are in terms of the lower heating value (LHV). The costs of water for electrolysis are not taken into account in this analysis as they are negligible in Germany. Finally, OPEX are always stated as % of CAPEX.

Table SI.2: General assumptions

	Value
Average transportation distance (one-way) [17, 18]	250 km
Average transportation speed [18]	50 km/h
Interest rate	4 %
Loading (LOHC) [19]	6.2 °weight-%
LOHC costs <sup>a</sup> [20]	4 €/kg <sub>LOHC</sub>

a: LOHC has a degradation rate of  $2 \times 0.1$  % (hydrogenation & dehydrogenation) [20] per supply-cycle, entailing additional costs of 0.13 €/kg. We interpret these costs as LOHC rental rate.

Table SI.3: Assumptions for different electrolysis technologies for 2030

	ALK	PEM
CAPEX (€/kW <sub>el</sub> ) <sup>a</sup> [10, 21]	550	724
OPEX (%) [22]	1.5	1.5
Depreciation period (a) <sup>a, d</sup> [21, 22]	10	10
Efficiency (%) <sup>c</sup> [22]	66	71
Pressure out (bar) [21, 22, 23]	30	30
Scale advantage (%) <sup>b</sup> [10]	20	20

a: Based on a 10 MW<sub>el</sub> electrolysis system with 2 times the current R&D investment and production scale-up.

b: Cost advantage when scaling up from 2.2 MW<sub>el</sub> to 10 MW<sub>el</sub>. The output of a 2.2 MW<sub>el</sub> and 10 MW<sub>el</sub> electrolyzer with an efficiency of 68.5 % (the center of our assumptions for ALK and PEM) is equal to 45 kg/h and 206 kg/h, respectively.

c: At the system level, incl. power supply, system control, gas drying (purity at least 99.4 %). Excl. external compression, external purification and hydrogen storage.

d: 60,000 h operation at an utilization rate of 70 %.

Table SI.4: Assumptions for different storage preparation processes (production site)

	GH <sub>2</sub> (D)	GH <sub>2</sub> (C)	GH <sub>2</sub> <sup>cav.</sup> (C)	LH <sub>2</sub> (C)	LOHC (C)
		<a href="#">[24]</a>	<a href="#">[24]</a>	<a href="#">[25]</a>	<a href="#">[18, 19, 20, 26, 27]</a>
Activity	-	compression	compression	liquefaction	hydrogenation
CAPEX-base (€)	-	40,528	40,528	643,700	74,657 <a href="#">[19]</a>
CAPEX-comparison	-	1 kW <sub>el</sub>	1 kW <sub>el</sub>	1 kg	1 kg
Scale	-	0.4603	0.4603	2/3	2/3
Ref.-Capacity (kg/h)	-	206	206	1030	1030
CAPEX-scaled (€/kg) <sup>a</sup>	-	2,923	2,672	63,739	7,392 <a href="#">[19]</a>
OPEX (%)	-	4	4	4	4
Depreciation period (a)	-	15	15	30	20
Pressure in (bar)	-	30	30	30 (20 nec.)	30
Pressure out (bar)	-	250	180	2	-
Compression stages	-	2	2	-	-
Elec. Demand (kWh/kg)	-	1.707	1.402	6.78	0.37
Heat Demand (kWh/kg)	-	-	-	-	-8.9
Losses (%)	-	0.5	0.5	1.625	3

*Abbreviations:* cav.: cavern; (D): decentralized supply chain; (C): centralized supply chain

a: For 10 MW<sub>el</sub> (206 kg/h) electrolysis capacity, the maximum daily throughput is almost 5 t of hydrogen. For non-stacked processes such as liquefaction and hydrogenation, we assume a throughput of 1030 kg/h which would be equal to the hydrogen production of a 50 MW<sub>el</sub> electrolyzer.

Table SI.5: Assumptions for different storage types (production site)

	GH <sub>2</sub> (D)	GH <sub>2</sub> (C)	GH <sub>2</sub> <sup>cav.</sup> (C)	LH <sub>2</sub> (C)	LOHC (C)
		<a href="#">[28]</a>	<a href="#">[29]</a>	<a href="#">[30]</a>	<a href="#">[18]</a>
CAPEX-base (€)	-	450	3.5	13.31	10
CAPEX-comparison	-	1 kg	1 kg	1 kg	1 kg
Scale	-	1	1	1	1
CAPEX-scaled (€/kg)	-	450	3.5	13.31	10
OPEX (%) <a href="#">[18]</a>	-	2	2.5 <a href="#">[31]</a>	2	2
Depreciation period (a) <a href="#">[28]</a>	-	20	30 <a href="#">[31]</a>	20	20
Pressure range (bar)	-	15 - 250	60 - 180	-	-
Min. filling level (%) <sup>a</sup>	-	6	33.3	5	-
Boil-off (%/d) <a href="#">[32]</a>	-	-	-	0.2	-
Storage bypass possibility	-	yes	yes	-	-

*Abbreviations:* cav.: cavern; (D): decentralized supply chain; (C): centralized supply chain

a: Calculated according to Boyle's law in order to maintain the minimum pressure required. For the cavern, minimum pressure is calculated dependent on the required amount of cushion gas.



Table SI.6: Assumptions for different transportation preparation processes

	GH <sub>2</sub> (D)	GH <sub>2</sub> (C) [24]	GH <sub>2</sub> <sup>cav.</sup> (C) [24]	LH <sub>2</sub> (C)	LOHC (C)
Activity	-	compression	compression	overflow/pumping	
CAPEX-base (€)	-	6000	6000	-	-
CAPEX-comparison	-	1 kW <sub>el</sub>	1 kW <sub>el</sub>	-	-
Scale	-	1	1	-	-
Ref.-Capacity (kg/h)		720	720	-	-
CAPEX-scaled (€/kg) <sup>a</sup>	-	13,784	6,530	-	-
OPEX (%)	-	4	4	-	-
Depreciation period (a)	-	15	15	-	-
Min. Pressure in (bar)	-	15	60	-	-
Pressure out (bar)	-	250	250	-	-
Compression stages	-	2	2	-	-
Elec. demand (kWh/kg)	-	2.297	1.088	-	-
Losses (%)	-	0.5	0.5	-	-

Abbreviations: cav.: cavern; (D): decentralized supply chain; (C): centralized supply chain

a: 720 kg/h is equal to the trailer capacity. Thus, every compressor is required to have the capacity to load one truck per hour.

Table SI.7: Assumptions for different transportation processes

	All [20]	GH <sub>2</sub> (C) [30]	LH <sub>2</sub> (C) [30]	LOHC (C) [18]
Function	tractor	trailer	trailer	trailer
CAPEX (€) <sup>a, b</sup>	223,031	518,400	865,260	150,000
Capacity (kg)	-	720	4,554	1,800
Net capacity (kg) <sup>c</sup>	-	676.8	4,326	1,620
CAPEX-net (€/kg)	-	763.93	190	92.59
OPEX (%)	12	2	2	2
Depreciation period (a) [20]	12	12	12	12
Losses (%/d) [32]	-	-	0.6	-
(Un-)/Loading time (h)	-	1 / 1	1 / 1	1 / 1

Abbreviations: (C): centralized supply chain

a: CAPEX adjusted for a lifetime of 12 years with an interest rate of 4 %.

b: The average fuel consumption of a tractor is assumed to be 35 L/100 km [20]. Moreover, we assume a price of 1.30 €/L for diesel and an hourly wage of drivers of 35 €. Fuel is not covered by the CO<sub>2</sub> tax.

c: For GH<sub>2</sub>, net-capacity is determined by the required outlet pressure. 5 % of LH<sub>2</sub> remain in the trailer to avoid heating up of the trailer-tank. For LOHC, a maximum discharge-depth of 90 % is assumed [19]. Thus, transportation capacity of actually usable hydrogen is below the total amount of bound hydrogen. For all other processes, issues linked to a discharge-depth below 100 % are ignored either because the effect on costs is negligible (storage, degradation) or because we assume a heat-recovery system being installed (dehydrogenation).

Table SI.8: Assumptions for different filling storage preparation processes (1<sup>st</sup> stage)

	GH <sub>2</sub> (D)	GH <sub>2</sub> (C) <a href="#">[24]</a>	LH <sub>2</sub> (C)	LOHC (C)
Activity	-	compression	overflow/pumping	
CAPEX-base (€)	-	40,035	-	-
CAPEX-comparison	-	1 kW <sub>el</sub>	-	-
Scale	-	0.6038	-	-
Ref.-Capacity (kg/h)	-	676.8	-	-
CAPEX-scaled (€/kg)	-	4,744	-	-
OPEX (%)	-	4	-	-
Depreciation period (a)	-	15	-	-
Pressure in (bar)	-	15	-	-
Pressure out (bar)	-	250	-	-
Compression stages <a href="#">[18]</a>	-	4	-	-
Elec. demand (kWh/kg)	-	2.105	-	-
Constraint (trailers/h) <sup>a</sup>	-	1	1	1
Losses (%)	-	0.5	2.5	-

*Abbreviations:* (D): decentralized supply chain; (C): centralized supply chain  
a: Own assumption to avoid congestion at the filling station.

Table SI.9: Assumptions for different storage technologies (1<sup>st</sup> stage)

	GH <sub>2</sub> (D)	GH <sub>2</sub> (C) <a href="#">[28]</a>	LH <sub>2</sub> (C) <a href="#">[30]</a>	LOHC (C) <a href="#">[18]</a>
CAPEX-base (€)	-	450	13.31	10
CAPEX-comparison	-	1 kg	1 kg	1 kg
Scale	-	1	1	1
CAPEX-scaled (€/kg)	-	450	13.31	10
OPEX (%) <a href="#">[18]</a>	-	2	2	2
Depreciation period (a) <a href="#">[28]</a>	-	20	20	20
Pressure range (bar)	-	15 - 250	-	-
Min. filling level (%) <sup>a</sup>	-	6	5	-
Boil-off (%/d) <a href="#">[32]</a>	-	-	0.4	-
Storage bypass possibility	-	yes	-	-

*Abbreviations:* (D): decentralized supply chain; (C): centralized supply chain  
a: Calculated according to Boyle's law in order to maintain the minimum pressure required.

Table SI.10: Assumptions for different filling storage preparation processes (2<sup>nd</sup> stage)

Activity	GH <sub>2</sub> (D)	GH <sub>2</sub> (C)	LH <sub>2</sub> (C)	LH <sub>2</sub> (C)	LOHC (C)	LOHC (C)
CAPEX-base (€)	<a href="#">[24]</a> compression 40,035	<a href="#">[24]</a> compression 40,035	<a href="#">[14]</a> <a href="#">[24]</a> cryo-compr.-pump 567.1 €/kg + 11,565 €	<a href="#">[14]</a> <a href="#">[24]</a> evaporation 900.9 €/kg + 2,389 €	<a href="#">[18]</a> <a href="#">[19]</a> <a href="#">[20]</a> <a href="#">[26]</a> <a href="#">[27]</a> dehydrogenation 55,707	<a href="#">[24]</a> compression 40,035
CAPEX-comparison	1 kW <sub>el</sub>	1 kW <sub>el</sub>	1 kg	1 kg	1 kg	1 kW <sub>el</sub>
Scale	0.6038	0.6038	1	1	2/3	0.6038
Ref.-Capacity (kg/h)	45	45	45	45	45	45
CAPEX-scaled (€/kg)	17,014	19,070	824.1	954	15,662	22,220
OPEX (%)	4	4	4	1	4	4
Depreciation period (a)	10	10	10	10	20	10
Pressure in (bar)	30	15	2	-	-	5 <a href="#">[19]</a>
Pressure out (bar)	950	950	-	950	5	950
Compression stages <a href="#">[18]</a>	4	4	-	-	-	4
Elec. demand (kWh/kg)	2.947	3.559	0.1 <a href="#">[18]</a>	0.6 <a href="#">[18]</a>	-	4.585
Heat demand (kWh/kg) <sup>a</sup>	-	-	-	-	9.1	-
Losses (%)	0.5	0.5	-	-	1	0.5

Abbreviations: (D): decentralized supply chain; (C): centralized supply chain  
a: 8.9 kWh/kg [\[18\]](#) [\[27\]](#) corrected for 97.5% heat exchanger efficiency as described in [\[19\]](#).

Table SI.11: Assumptions for different storage technologies (2<sup>nd</sup> stage)

	All <a href="#">[30]</a>
CAPEX-base (€)	600
CAPEX-comparison	1 kg
Scale	1
CAPEX-scaled (€/kg)	600
OPEX (%)	2
Depreciation period (a)	20
Pressure range (bar)	700 - 950
Min. filling level (%) <sup>a</sup>	74

a: Calculated according to Boyle's law in order to maintain the minimum pressure required. For the cavern, minimum pressure is calculated dependent on the required amount of cushion gas.

Table SI.12: Assumptions for filling station equipment

	Refrigeration <a href="#">[24]</a>	Dispenser <a href="#">[24]</a>
CAPEX-base (€/pc.) <a href="#">[30]</a>	70,000	60,000
OPEX (%)	2	1
Depreciation period (a)	15	10
Elec. demand (kWh/kg)	0.325	-
Max. temperature (°C) <sup>a</sup>	-40	-40

a: Hydrogen is dispensed to cars in gaseous form at 700 bar and pre-cooled to  $-40^{\circ}\text{C}$  in order to guarantee short filling times [\[24\]](#).

Table SI.13: Sensitivity: mass storage for decentralized electrolysis

	GH <sub>2</sub> (D) <a href="#">[24]</a>	GH <sub>2</sub> (D) <a href="#">[24]</a>
Activity	compression (mass storage)	compression (high pressure storage)
CAPEX-base (€)	40,035	40,035
CAPEX-comparison	1 kW <sub>el</sub>	1 kW <sub>el</sub>
Scale	0.6038	0.6038
Ref.-Capacity (kg/h)	45	45
CAPEX-scaled (€/kg)	11,972	17,014
OPEX (%)	4	4
Depreciation period (a)	15	10
Pressure in (bar)	30	30
Pressure out (bar)	250	950
Compression stages <a href="#">[18]</a>	4	4
Elec. demand (kWh/kg)	1.654	2.947
Losses (%)	0.5	0.5

Abbreviations: (D): decentralized supply chain

## SI References

- [1] P. Preuster, C. Papp, and P. Wasserscheid. Liquid Organic Hydrogen Carriers (LOHCs): Toward a Hydrogen-Free Hydrogen Economy. *Accounts of Chemical Research*, 50(1):74–85, 2017. [doi:10.1021/acs.accounts.6b00474](https://doi.org/10.1021/acs.accounts.6b00474).
- [2] Bundesnetzagentur. Genehmigung des Szenariorahmens 2019-2030, 2018. Available at: [https://www.netzentwicklungsplan.de/sites/default/files/paragraphs-files/Szenariorahmen\\_2019-2030\\_Genehmigung\\_0\\_0.pdf](https://www.netzentwicklungsplan.de/sites/default/files/paragraphs-files/Szenariorahmen_2019-2030_Genehmigung_0_0.pdf) [last accessed: Apr. 6, 2020].
- [3] A. Schröder, F. Kunz, J. Meiss, R. Mendelevitch, and C. von Hirschhausen. Current and Prospective Costs of Electricity Generation until 2050. Data Documentation 68, DIW Berlin, 2013. Available at: [https://www.diw.de/documents/publikationen/73/diw\\_01.c.424566.de/diw\\_datadoc\\_2013-068.pdf](https://www.diw.de/documents/publikationen/73/diw_01.c.424566.de/diw_datadoc_2013-068.pdf) [last accessed: Apr. 6, 2020].
- [4] C. Pape, N. Gerhardt, P. A. Härtel, Scholz, T. Schwinn, R. and Drees, A. Maaz, J. Sprey, C. Breuer, A. Moser, F. Sailer, S. Reuter, and T. Müller. Roadmap Speicher. Commissioned by: BMWi, 2014. Available at: [https://www.iee.fraunhofer.de/content/dam/iee/energiesystemtechnik/de/Dokumente/Studien-Reports/2014\\_Roadmap-Speicher-Langfassung.pdf](https://www.iee.fraunhofer.de/content/dam/iee/energiesystemtechnik/de/Dokumente/Studien-Reports/2014_Roadmap-Speicher-Langfassung.pdf) [last accessed: Apr. 6, 2020].
- [5] O. Schmidt, A. Hawkes, A. Gambhir, and I. Staffell. The Future Cost of Electrical Energy Storage Based on Experience Rates. *Nature Energy*, 2, 2017. [doi:10.1038/nenergy.2017.110](https://doi.org/10.1038/nenergy.2017.110).
- [6] ENTSO-E. Maps & Data for the Ten Year Network Development Plan 2018. Technical report, European Network of Transmission System Operators for Electricity, 2018. Available at: <https://tyndp.entsoe.eu/maps-data/> [last accessed: Apr. 6, 2020].
- [7] S. Pfenninger and I. Staffell. Long-Term Patterns of European PV Output Using 30 Years of Validated Hourly Reanalysis and Satellite Data. *Energy*, 114:1251–1265, 2016. [doi:10.1016/j.energy.2016.08.060](https://doi.org/10.1016/j.energy.2016.08.060).
- [8] I. Staffell and S. Pfenninger. Using Bias-Corrected Reanalysis to Simulate Current and Future Wind Power Output. *Energy*, 114:1224–1239, 2016. [doi:10.1016/j.energy.2016.08.068](https://doi.org/10.1016/j.energy.2016.08.068).
- [9] A. Zerrahn, W.-P. Schill, and F. Stöckl. DIETER Model Version for the Paper “Optimal Hydrogen Supply Chains: Co-Benefits for Integrating Renewable Energy Sources”. Zenodo, 2020. [doi:10.5281/zenodo.3693306](https://doi.org/10.5281/zenodo.3693306).
- [10] H. G. Langås. Large Scale Hydrogen Production. NEL, 2015. Available at: <https://www.sintef.no/contentassets/9b9c7b67d0dc4fbf9442143f1c52393c/9-hydrogen-production-in->

- 
- [large-scale-henning-g.-langas-nel-hydrogen.pdf](#) [last accessed: Apr. 6, 2020].
- [11] M. Schubert, T. Kluth, G. Nebauer, R. Ratzenberger, S. Kotzagiorgis, B. Butz, W. Schneider, and M. Leible. Verkehrsverflechtungsprognose 2030. Schlussbericht. Los 3: Erstellung der Prognose der deutschlandweiten Verkehrsverflechtungen unter Berücksichtigung des Luftverkehrs. Commissioned by: BMVI, 2014. Available at: <http://daten.clearingstelle-verkehr.de/276/1/verkehrsverflechtungsprognose-2030-schlussbericht-los-3.pdf> [last accessed: Apr. 6, 2020].
- [12] H. Hass, A. Huss, and H. Maas. Tank-to-Wheels Report Version 4.a. Technical report, European Commission, 2014. Available at: [http://publications.jrc.ec.europa.eu/repository/bitstream/JRC85327/ttw\\_report\\_v4a\\_online.pdf](http://publications.jrc.ec.europa.eu/repository/bitstream/JRC85327/ttw_report_v4a_online.pdf) [last accessed: Apr. 6, 2020].
- [13] S. Radke. *Verkehr in Zahlen 2017/2018*. DVV Media Group, Hamburg, 2017.
- [14] Nexant, Inc., Air Liquide, Argonne National Laboratory, Chevron Technology Venture, Gas Technology Institute, National Renewable Energy Laboratory, Pacific Northwest National Laboratory, and TIAx LLC. H<sub>2</sub>A Hydrogen Delivery Infrastructure Analysis Models and Conventional Pathway Options Analysis Results - Interim Report. Commissioned by: US-DOE, 2008. Available at: [https://www.energy.gov/sites/prod/files/2014/03/f9/nexant\\_h2a.pdf](https://www.energy.gov/sites/prod/files/2014/03/f9/nexant_h2a.pdf) [last accessed: Apr. 6, 2020].
- [15] US-EIA. Prime Supplier Sales Volumes, 2018. Available at: [https://www.eia.gov/dnav/pet/pet\\_cons\\_prim\\_dcu\\_nus\\_m.htm](https://www.eia.gov/dnav/pet/pet_cons_prim_dcu_nus_m.htm) [last accessed: Apr. 6, 2020].
- [16] H2Mobility. 70MPa Hydrogen Refuelling Station Standardization - Function Description of Station Modules. *Mimeo*, 2010.
- [17] P. Runge, C. Sölch, J. Albert, P. Wasserscheid, G. Zöttl, and V. Grimm. Economic Comparison of Different Electric Fuels for Energy Scenarios in 2035. *Applied Energy*, 233-234:1078–1093, 2019. doi:10.1016/j.apenergy.2018.10.023.
- [18] M. Reuß, T. Grube, M. Robinius, P. Preuster, P. Wasserscheid, and D. Stolten. Seasonal Storage and Alternative Carriers: A Flexible Hydrogen Supply Chain Model. *Applied Energy*, 200:290–302, 2017. doi:10.1016/j.apenergy.2017.05.050.
- [19] M. Eypasch, M. Schimpe, A. Kanwar, T. Hartmann, S. Herzog, T. Frank, and T. Hamacher. Model-Based Techno-Economic Evaluation of an Electricity Storage System Based on Liquid Organic Hydrogen Carriers. *Applied Energy*, 185:320–330, 2017. doi:10.1016/j.apenergy.2016.10.068.

- [20] D. Teichmann, W. Arlt, and P. Wasserscheid. Liquid Organic Hydrogen Carriers as an Efficient Vector for the Transport and Storage of Renewable Energy. *International Journal of Hydrogen Energy*, 37(23):18118–18132, 2012. [doi:10.1016/j.ijhydene.2012.08.066](https://doi.org/10.1016/j.ijhydene.2012.08.066).
- [21] O. Schmidt, A. Gambhir, I. Staffell, A. Hawkes, J. Nelson, and S. Few. Future Cost and Performance of Water Electrolysis: An Expert Elicitation Study. *International Journal of Hydrogen Energy*, 42(52):30470–30492, 2017. [doi:10.1016/j.ijhydene.2017.10.045](https://doi.org/10.1016/j.ijhydene.2017.10.045).
- [22] L. Bertuccioli, A. Chan, D. Hart, F. Lehner, B. Madden, and E. Standen. Development of Water Electrolysis in the European Union. Commissioned by: Fuel Cells and Hydrogen Joint Undertaking, 2014. Available at: [https://www.fch.europa.eu/sites/default/files/study%20electrolyser\\_0-Logos\\_0\\_0.pdf](https://www.fch.europa.eu/sites/default/files/study%20electrolyser_0-Logos_0_0.pdf) [last accessed: Apr. 6, 2020].
- [23] M. Carmo, D. L. Fritz, J. Mergel, and D. Stolten. A Comprehensive Review on PEM Water Electrolysis. *International Journal of Hydrogen Energy*, 38(12):4901–4934, 2013. [doi:10.1016/j.ijhydene.2013.01.151](https://doi.org/10.1016/j.ijhydene.2013.01.151).
- [24] A. Elgowainy, K. Reddi, M. Mintz, and D. Brown. H2A Delivery Scenario Analysis, Model Version 3.0 (HDSAM 3.0), 2015. Available at: <https://hdsam.es.anl.gov/index.php?content=hdsam> [last accessed: Apr. 6, 2020].
- [25] K. Stolzenburg and R. Mubbala. Integrated Design for Demonstration of Efficient Liquefaction of Hydrogen (IDEALHY). Commissioned by: Fuel Cells and Hydrogen Joint Undertaking, 2013. Available at: [https://www.idealhy.eu/uploads/documents/IDEALHY\\_D3-16\\_Liquefaction\\_Report\\_web.pdf](https://www.idealhy.eu/uploads/documents/IDEALHY_D3-16_Liquefaction_Report_web.pdf) [last accessed: Apr. 6, 2020].
- [26] A. W. McClaine, K. Brown, and D. D. G. Bowen. Magnesium Hydride Slurry: A Better Answer to Hydrogen Storage. *Journal of Energy Resources Technology*, 137(6):06120101–06120109, 2015. [doi:10.1115/1.4030398](https://doi.org/10.1115/1.4030398).
- [27] K. Müller, K. Stark, V. N. Emel’yanenko, M. A. Varfolomeev, D. H. Zaitsau, E. Shoifet, C. Schick, S. P. Verevkin, and W. Arlt. Liquid Organic Hydrogen Carriers: Thermophysical and Thermochemical Studies of Benzyl- and Dibenzyl-toluene Derivatives. *Industrial & Engineering Chemistry Research*, 54(32):7967–7976, 2015. [doi:10.1021/acs.iecr.5b01840](https://doi.org/10.1021/acs.iecr.5b01840).
- [28] G. Parks, R. Boyd, J. Cornish, and R. Remick. Hydrogen Station Compression, Storage, and Dispensing Technical Status and Costs: Systems Integration. NREL Technical Report, 2014. Available at: <https://www.hydrogen.energy.gov/pdfs/58564.pdf> [last accessed: Apr. 6, 2020].
- [29] O. Kruck, F. Crotogino, R. Prelicz, and T. Rudolph. Assessment of the Potential, the Actors and Relevant Business Cases for Large Scale and Seasonal Storage of Renewable Electricity by Hydrogen Underground Storage in Europe. Commissioned by: Fuel Cells and Hydrogen Joint Undertaking, 2013.

Available at: [http://hyunder.eu/wp-content/uploads/2016/01/D3.1\\_Overview-of-all-known-underground-storage-technologies.pdf](http://hyunder.eu/wp-content/uploads/2016/01/D3.1_Overview-of-all-known-underground-storage-technologies.pdf) [last accessed: Apr. 6, 2020].

- [30] US-DOE. Hydrogen Delivery. In US-DOE, editor, *Fuel Cell Technologies Program Multi-Year Research, Development, and Demonstration Plan (MYRD&D Plan)*, chapter 3.2. US-DOE, 2015. Available at: <https://www.energy.gov/eere/fuelcells/downloads/fuel-cell-technologies-office-multi-year-research-development-and-22> [last accessed: Apr. 6, 2020 – subject to updates].
- [31] K. Stolzenburg, R. Hamelmann, M. Wietschel, F. Genoese, J. Michaelis, J. Lehmann, A. Miede, S. Krause, C. Sponholz, S. Donadei, F. Crocogino, A. Acht, and P.-L. Horvath. Integration von Wind-Wasserstoff-Systemen in das Energiesystem. Commissioned by: BMVI, 2014. Available at: [https://www.now-gmbh.de/content/1-aktuelles/1-presse/20140402-abschlussbericht-zur-integration-von-wind-wasserstoff-systemen-in-das-energiesystem-ist-veroeffentlicht/abschlussbericht\\_integration\\_von\\_wind-wasserstoff-systemen\\_in\\_das\\_energiesystem.pdf](https://www.now-gmbh.de/content/1-aktuelles/1-presse/20140402-abschlussbericht-zur-integration-von-wind-wasserstoff-systemen-in-das-energiesystem-ist-veroeffentlicht/abschlussbericht_integration_von_wind-wasserstoff-systemen_in_das_energiesystem.pdf) [last accessed: Apr. 6, 2020].
- [32] N. Bouwkamp, A. Burgunder, D. Casey, A. Elgowainy, L. Fisher, J. Merritt, E. Miller, A. Petitpas, G. and Rohatgi, N. Rustagi, J. Simnick, H. Soto, and J. Vickers. Hydrogen Delivery Technical Team Roadmap. Commissioned by: US DRIVE Partnership, 2017. Available at: [https://www.energy.gov/sites/prod/files/2017/08/f36/hdtt\\_roadmap\\_July2017.pdf](https://www.energy.gov/sites/prod/files/2017/08/f36/hdtt_roadmap_July2017.pdf) [last accessed: Apr. 6, 2020].